

~~CONFIDENTIAL~~

6

Copy  
RM E52J07

JUN 3 1953



## RESEARCH MEMORANDUM

ALTITUDE PERFORMANCE INVESTIGATION OF TWO SINGLE-ANNULAR  
TYPE COMBUSTORS AND THE PROTOTYPE J40-WE-8 TURBOJET  
ENGINE COMBUSTOR WITH VARIOUS COMBUSTOR-INLET  
AIR PRESSURE PROFILES

By Adam E. Sobolewski, Robert R. Miller, and John E. McAulay

Lewis Flight Propulsion Laboratory

CLASSIFICATION ~~CHANGED~~ Ohio

UNCLASSIFIED

To \_\_\_\_\_

By authority of *NACA Rec Adm*  
*LRN-124* Date *Apr. 20, 1958*

*Amc 2-12-58*

CLASSIFIED DOCUMENT

This material contains information affecting the National Defense of the United States within the meaning of the espionage laws, Title 18, U.S.C., Secs. 793 and 794, the transmission or revelation of which in any manner to an unauthorized person is prohibited by law.

NATIONAL ADVISORY COMMITTEE  
FOR AERONAUTICS

WASHINGTON

May 29, 1953

NACA LIBRARY

LANGLEY AERONAUTICAL LABORATORY  
Langley Field, Va.

~~CONFIDENTIAL~~

NACA RM E52J07

## NATIONAL ADVISORY COMMITTEE FOR AERONAUTICS

RESEARCH MEMORANDUMALTITUDE PERFORMANCE INVESTIGATION OF TWO SINGLE-ANNULAR TYPE  
COMBUSTORS AND THE PROTOTYPE J40-WE-8 TURBOJET ENGINE COMBUSTOR  
WITH VARIOUS COMBUSTOR INLET-AIR PRESSURE PROFILES

By Adam E. Sobolewski, Robert R. Miller, and John E. McAulay

## SUMMARY

Data were obtained for three single-annular type combustors with different combustor inlet-air pressure profiles over a range of engine speeds at an altitude of 30,000 feet and a flight Mach number of 0.62. The combustors with a lower percentage of total hole area at the inner wall had a higher combustor-outlet temperature profile near the inner wall than the combustor with equal hole-area distributions; the converse was true near the outer wall. As the combustor inlet-air pressure profile was lowered (corresponding to a reduction in air flow) at the inner portion of the passage height, the combustor-outlet temperature profile near the inner wall was raised. Similar trends were encountered near the outer wall. Combustor pressure-loss coefficient was not affected by hole-area distribution but was affected by total hole area and inlet-air pressure profile. For combustors with total hole areas of 877 and 809 square inches, the pressure-loss coefficients were 10.8 and 12.4, respectively, at a combustor density ratio of 2.2. For changes in inlet-air pressure profile, the pressure-loss coefficient varied from 10.8 to 15.8, at a density ratio of 2.2. There was no discernible effect of the aforementioned variables on combustion efficiency.

Combustor performance data were also obtained with the compressor-combustor configuration of the turbojet engine designated the prototype J40-WE-8. These data were obtained over a range of altitudes from 15,000 to 55,000 feet and flight Mach numbers from 0.17 to 0.99. For the prototype J40-WE-8 turbojet-engine combustor, combustion efficiency at a corrected engine speed of 7600 rpm decreased from 0.98 at an altitude of 15,000 feet to 0.83 at an altitude of 55,000 feet at a flight Mach number of 0.62 and open exhaust-nozzle area (area of 534 sq in.).

A good correlation was obtained when combustion efficiency was presented as a function of a combustion parameter and engine fuel-air ratio. These data indicated that at values of combustion parameter below 34,000 pounds-°R-second per cubic foot there was a fuel-air ratio that resulted in an optimum combustion efficiency for a given value of combustion parameter.

## INTRODUCTION

An investigation of the performance of the XJ40-WE-6 turbojet engine in the NACA Lewis altitude wind tunnel disclosed that the engine operated with compressor surge and a combustor-outlet temperature inversion within the desired operating speed range. As a result of changes made in the setting of the blades in the compressor and a study of the configuration of the combustor, conducted in cooperation with the engine manufacturer, the compressor surge was displaced out of the operating speed range and the combustor-outlet temperature inversion was corrected. These results are reported in references 1 and 2.

In correcting the combustor-outlet temperature inversion, three single-annular-type combustors having slightly different air-passage geometry were evaluated on the engine. Correcting the compressor surge by making changes to the blade settings resulted in different inlet-air pressure profiles at the inlet to the combustors and made possible a determination of the effect of inlet-air pressure profile on combustor performance. This investigation was conducted over a range of engine speeds, at an altitude of 30,000 feet, and a flight Mach number of 0.65.

The XJ40-WE-6 engine having the improved compressor and combustion-chamber configuration was designated the prototype J40-WE-8 turbojet engine without an afterburner. Combustor performance data on the prototype J40-WE-8 engine were obtained over a range of altitudes from 15,000 to 55,000 feet, flight Mach numbers from 0.17 to 0.99, and over a range of engine speeds at five fixed exhaust-nozzle areas. These combustor data constituted the first evaluation in an altitude facility of the performance of a single-annular combustor with spring-loaded variable-area fuel nozzles operating as an integral component of a turbojet engine.

Combustor data are presented herein to show the correlation of combustion efficiency with engine fuel-air ratio and a combustion parameter expressed in terms of inlet variables  $P_4 T_4 / V_p$ . (All symbols used in this report are given in appendix A.)

The performance of the prototype J40-WE-8 turbojet-engine combustor and three other different types of combustors are compared herein by data which shows the variation of combustion efficiency with fuel-air ratio and combustion parameter  $P_4 T_4 / V_b$  for the different combustors.

## APPARATUS

### Engine

The turbojet engine used at the start of this investigation was designated the XJ40-WE-6. Subsequent compressor and combustor configurations resulted in the prototype J40-WE-8 turbojet engine without afterburner (fig. 1). A manufacturer's rating for the prototype J40-WE-8 turbojet engine is not available at the present time; however, its rating would be similar to the rating of the XJ40-WE-6 turbojet engine, which had a static sea-level thrust of 7500 pounds at an engine speed of 7260 rpm and a turbine-inlet temperature of  $1425^{\circ}\text{F}$  ( $1885^{\circ}\text{R}$ ). At this operating condition the air flow was approximately 142 pounds per second, and the combustor-inlet total pressure, total temperature, and velocity (based on the maximum cross-sectional area of the combustor, 6.40 sq ft) were 10,600 pounds per square foot absolute,  $870^{\circ}\text{R}$ , and 101 feet per second, respectively. The principal components of the engine were an eleven-stage axial-flow compressor, single-annular combustor, two-stage turbine, diffuser, and variable-area exhaust nozzle.

A number of different compressor configurations were obtained in the compressor development program, and data were selected for presentation herein from three configurations. These configurations, which were designated compressors 1 to 3, were chosen because they provided a wide range of combustor inlet-air pressure profiles.

### Combustors

Combustion data were obtained with three combustors (supplied by the manufacturer) which were of the single-annular type, differing only in the perforations in the inner and outer walls of the combustor basket and in some mechanical strengthening features. These combustors had a maximum cross-sectional area of 6.40 square feet. The combustors, designated A, B, and C, are shown in figures 2, 3, and 4, respectively. A cross section of the combustors and a developed sketch of an element of surface from the combustor baskets for each of the three combustors are shown in figure 5. The variation of total hole area with combustor length for the three combustors is presented in figure 6. The total hole area includes the area of the

openings shown in figure 5 and the various circumferential openings located at the inner and outer walls of the combustor. As shown in figure 6, the total hole area for combustors A and C was 796 and 877 square inches, respectively; however, approximately the same percentage of hole area was provided at the inner and outer walls of the combustor basket. The distribution of total hole area was 46.5 percent at the inner wall and 53.5 percent at the outer wall. Combustor B, which had a total hole area approximately the same as combustor A, had equal area distribution at the inner and outer walls of the combustor basket.

The splitter (fig. 5) divided the air flow entering the combustor into two annular passages formed by the combustor basket and the inner and outer walls of the combustor. Engine fuel was admitted and sprayed downstream in the combustor through 16 spring-loaded variable-area nozzles located at the upstream end of the combustor. Through the combined action of an engine-fuel distributor, equalizing valves, and spring-loaded variable-area nozzles, the fuel flow through each of the 16 nozzles was maintained equal at all fuel flows.

#### INSTALLATION AND INSTRUMENTATION

The engine was mounted on a wing section that spanned the 20-foot-diameter test section of the altitude wind tunnel (fig. 1). Dry refrigerated air was supplied to the engine from the tunnel make-up air system through a duct connected to the engine inlet. Throttle valves were installed in the duct to permit regulation of the pressure at the inlet of the engine. Instrumentation for measuring pressures and temperatures was installed at various stations in the engine (figs. 7 and 8). Ten sonic probe thermocouples, which could be traversed radially, were used at the combustor-outlet station (fig. 8(c)) to obtain temperature profiles.

#### PROCEDURE

Dry refrigerated air was supplied to the engine at the standard temperature for each flight condition with the exception that the minimum temperature obtained was about  $-20^{\circ}\text{F}$  ( $440^{\circ}\text{R}$ ). The air, at approximately sea-level pressure at the entrance of the make-up air system, was throttled to a total pressure at the engine inlet corresponding to the desired flight condition, with complete free-stream ram pressure recovery assumed.

Combustor performance data, showing the effect of different combustor inlet-air pressure profiles and combustor hole-area

distribution on combustor performance, were obtained at an altitude of 30,000 feet, a flight Mach number of 0.62, and over a range of engine speeds.

The combustor of the prototype J40-WE-8 turbojet engine, which consisted of compressor 1 and combustor A, was investigated over a range of altitudes from 15,000 to 55,000 feet, flight Mach numbers from 0.17 to 0.99, at several constant exhaust-nozzle areas, and over a range of engine speeds.

Complete radial surveys of the combustor-outlet temperature using the sonic probe thermocouples were obtained at rated speed only. The engine fuel used was MIL-F-5624 at a temperature of about 80° F. This fuel had a lower heating value of 18,700 Btu per pound and a hydrogen to carbon ratio of 0.171. The methods of calculation are presented in appendix B.

## RESULTS AND DISCUSSION

### Effect of Changing Combustor Inlet-Air Pressure Profile and Hole Geometry on Combustor Performance

The effects on combustor performance of inlet-air pressure profiles and combustor hole-area distribution are discussed in terms of (1) temperature profile at the combustor outlet, (2) pressure-loss characteristics, and (3) combustion efficiency.

Combustor-outlet temperature profiles. - The effect of different combustor configurations on combustor-outlet temperature profiles for operating conditions at high and low engine speeds is shown in figures 9 and 10. As mentioned previously, radial temperature surveys at the combustor outlet (station 5, fig. 8(c)) were obtained only at rated speed. It has been shown, however, that turbine-outlet temperature profiles (station 6, fig. 8(d)) are indicative of turbine-inlet or combustor-outlet temperature profiles; therefore, turbine-outlet temperature profiles are presented at reduced engine speeds (fig. 9(d) and 10(d)). In the comparison of the combustor configurations the combustor inlet-air pressure profiles (compressor outlet-air pressure profiles) are the same. Any change in combustor performance may therefore be attributed to the difference in the combustor hole geometry. Combustors A and B, which are compared in figure 9, have about the same total hole area, but different hole-area distribution. The percentage hole-area distribution at the inner wall for combustors A and B was 46.5 and 50 percent, respectively. As shown in figure 9, the combustor-outlet temperature distribution was

affected by variations in hole-area distribution. The effect of changes in hole-area distribution at the inner and outer walls was to cause a radial shift (due to a restriction or damming effect) in air flow in the region between the compressor outlet, where the combustor inlet-air pressure profiles were measured, and the splitter (fig. 5). The decrease in hole area at the inner wall for combustor A resulted in lower air flow and, therefore, high combustor-outlet temperatures near the inner wall. Conversely, combustor A had relatively lower combustor-outlet temperatures near the outer wall.

The combustors compared in figure 10 differ both in hole-area distribution and total hole area. Combustor B had a total hole area of 809 square inches, 50 percent of which was located on the inner wall, and combustor C had a total hole area of 877 square inches, 46.5 percent of which was located on the inner wall. This lower percent of total hole area and air flow at the inner wall of combustor C resulted in higher combustor-outlet temperatures near the inner wall as shown in figures 10(b) and 10(d). The reverse was again true at the outer wall.

Although the changes in combustor-outlet temperature profile for the different combustors have been explained on the basis of total hole-area distribution at the inner and outer walls, the effect of changes in the axial hole distribution (figs. 5 and 6) is also an influencing factor. It was not possible, however, from the data available to account for the effect of changes in the axial hole distribution.

The effect of combustor inlet-air pressure profile on combustor-outlet temperature profile is shown in figure 11. The splitter located at the upstream end of the combustor (fig. 5) tends to direct the air flow in the inner 55 percent of the passage height towards the inner wall of the combustor and the remaining portion of the air flow towards the outer wall. As shown in figures 11(a) and 11(c) the shift in total-pressure distribution with change in compressor configuration resulted in a greater percentage of the total air flow for compressor 2 relative to compressor 3 to be directed towards the inner wall of the combustor. This effect resulted in lower combustor-outlet temperatures at the inner portion of the passage height and higher temperatures at the outer portion of the passage height for compressor 2 (figs. 11(b) and 11(d)). Thus, for the series of combustors investigated the combustor-outlet temperature profile was shown to be influenced by the combustor inlet-air pressure profile as well as by the changes in combustor hole-area distribution discussed previously.

2626

Pressure-loss characteristics. - The effect of combustor configurations and combustor inlet-air pressure profiles on combustor pressure-loss coefficient  $(P_4 - P_5)/q_p$  is presented in figure 12. Although there is considerable scatter in the data, particularly at low total density ratios, curves were faired through the points with the aid of trends established from data for other configurations and from wind-milling engine tests. Combustors A and B, compared in figure 12(a), have about the same total hole area but differ in hole-area distribution. As shown, in figure 12(a) there was no apparent difference in pressure loss between the two combustors. Combustors B and C, having different hole areas and hole distributions, are compared in figure 12(b). The pressure loss is greater for combustor B which had the smaller total hole area. At a constant value of combustor density ratio of 2.2, the pressure-loss coefficient was 10.8 and 12.4 for combustors C and B, respectively. The data show, therefore, that over the range of hole geometry investigated the pressure loss was independent of hole area distribution (fig. 12(a)) and dependent on the total hole area (fig. 12(b)).

The effect of combustor inlet-air pressure profile on combustor total-pressure-loss coefficient of combustor C is shown in figure 12(c). The pressure loss for the air-pressure profile of compressor 2 was greater than that obtained with compressor 3. At a density ratio of 2.2, the pressure-loss coefficient was 10.8 and 15.8 for air-pressure profiles of compressors 3 and 2, respectively. Since the temperature profiles shown in figures 11(b) and 11(d) indicate that compressor 2 directs a greater proportion of the air flow toward the combustor inner wall than compressor 3, and also that the combustor inner wall had a lower percentage of the total hole area than the outer wall, the pressure-loss coefficient would tend to be greater for the air-pressure profile of compressor 2. Thus, it is apparent that the pressure-loss coefficient is sensitive to combustor inlet-air pressure profile; however, it is not possible to determine precisely whether the increase in pressure-loss coefficient associated with compressor 2 was due entirely to the increase in losses in mixing and turbulence in the combustor basket or in diffusion loss from the combustor inlet (compressor outlet) to the combustor.

Combustion efficiency. - The effect of combustor configurations and combustor inlet-air pressure profiles on combustion efficiency is shown in figure 13. In order to enable a direct comparison of the different combustors and inlet-air pressure profiles irrespective of differences in inlet pressure, temperatures, or velocities, the combustion correlation parameter  $P_4 T_4 / V_p$  was used. This combustion parameter is derived in reference 3. As will be shown later, there was an additional effect of fuel-air ratio on combustion efficiency.

Inasmuch as the various configurations were investigated at the same flight conditions, and over the same range of engine speeds and exhaust-nozzle areas, the fuel-air ratios for each of the configurations were essentially the same for any given value of combustion parameter shown in figure 13. The data show that for the configurations and pressure profiles studied there was no effect of these variables on combustion efficiency. Combustion efficiency remained approximately constant at 0.98 for values of combustion parameter greater than 34,000 pounds- $^{\circ}$ R-second per cubic foot, and decreased for values of combustion parameter below 34,000 pounds- $^{\circ}$ R-second per cubic foot to 0.60 at a combustion parameter of 8400 pounds- $^{\circ}$ R-second per cubic foot.

#### Performance of the Prototype J40-WE-8 Turbojet-Engine Combustor

The results presented in the previous discussion were obtained during the early phase of the investigation which consisted of a compressor development and combustor evaluation program of the XJ40-WE-6 turbojet engine. From this part of the investigation, as mentioned previously, a configuration comprised of compressor 1 and combustor A was selected for the prototype J40-WE-8 turbojet engine. This configuration was chosen because of improved compressor surge characteristics, elimination of combustor-outlet temperature inversion (references 1 and 2), and satisfactory mechanical reliability of the combustor. A performance evaluation of this configuration was obtained over a wide range of flight and engine operating conditions and is presented in the following section. Most of the performance data are presented at an exhaust-nozzle area of 534 square inches (open nozzle). The trends of the data for all the exhaust-nozzle areas were similar, but the effects on the combustor performance were somewhat greater with the open exhaust-nozzle area. Data for all exhaust-nozzle areas are presented in table I.

Combustion efficiency. - The effects of corrected engine speed, altitude, flight Mach number, and exhaust-nozzle area on combustion efficiency are shown in figure 14. Although flight condition, engine speed, and exhaust-nozzle area are not basic combustor variables, the data in figure 14 are shown in order to illustrate the variation in performance of the combustor in an engine. The variations in combustion efficiency for a given combustor configuration are primarily due to changes in combustor-inlet pressure, temperature, velocity, and fuel-air ratio as will be discussed later. At a flight Mach number of 0.62 and exhaust-nozzle area of 534 square inches, combustion

efficiency decreased from 0.98 at 15,000 feet to 0.83 at 55,000 feet, at a corrected engine speed of 7600 rpm (fig. 14(a)). The effect of altitude on combustion efficiency becomes even more pronounced at the lower engine speeds. Although the variables, flight Mach number and exhaust nozzle area, also affect combustion efficiency, the effects are less pronounced than the altitude effect as shown in figures 14(b) and 14(c), respectively. At a corrected engine speed of 7600 rpm and at an altitude of 35,000 feet, (fig. 14(b)) a change in flight Mach number from 0.17 to 0.99, increased combustion efficiency from about 0.955 to 0.995. In figure 14(c), which shows the effect of exhaust-nozzle area on combustion efficiency at 35,000 feet and flight Mach number of 0.62, combustion efficiency increased from about 0.97 to 0.98 as the exhaust-nozzle area was reduced from 534 to 420 square inches at a corrected engine speed of 7600 rpm.

Combustor pressure-loss characteristics. - Combustor pressure-loss characteristics are presented in terms of engine parameters in figure 15 and of combustor parameters in figure 16. In both figures the pressure-loss characteristics include the pressure loss due to (1) the diffusion process from the combustor inlet (compressor outlet) to the combustor basket, (2) mixing and turbulence in the combustor basket, and (3) momentum pressure loss associated with the burning process. For all flight conditions and exhaust-nozzle areas, the combustor total-pressure-loss ratio  $(P_4 - P_5)/P_4$  decreased with increasing corrected engine speed above a corrected engine speed of about 6000 rpm (fig. 15). For example, at an altitude of 35,000 feet, flight Mach number of 0.62, and exhaust-nozzle area of 534 square inches, the combustor total-pressure-loss ratio decreased from 0.040 to 0.031 as corrected engine speed increased from 6000 to 7400 rpm (fig. 15). This reduction in pressure-loss ratio with increasing corrected engine speed may be attributed to a more favorable combustor inlet-air pressure profile resulting in a more efficient diffusion process. At a constant value of corrected engine speed, decreasing altitude (fig. 15(a)) or increasing flight Mach number (fig. 15(b)) or exhaust-nozzle area (fig. 15(c)), in general, resulted in an increasing pressure-loss ratio. For instance, at a corrected engine speed of 7000 rpm, altitude of 35,000 feet, and flight Mach number of 0.62, increasing exhaust-nozzle area from 367 to 534 square inches resulted in an increase of total-pressure-loss ratio from 0.024 to 0.036 (fig. 15(c)).

The combustor pressure-loss characteristics are presented in terms of fundamental combustor parameters in figure 16. The combustor total-pressure-loss coefficient increased as the combustor total-density ratio was increased from 1.0 to 1.9, reaching a maximum value of 9.2 at a density ratio of 1.9. For values of density ratios above 1.9, the pressure-loss coefficient tends to decrease. From theoretical considerations (reference 4), the pressure-loss coefficient should vary linearly with density ratio. Possible factors in the disagreement are that the

efficiency of the diffusion process, as well as the mixing and turbulent losses in the combustion, varied as the density ratio was changed.

### Correlation of Combustion Efficiency with Engine Fuel-Air Ratio and Combustion Parameter

Because the process of combustion is complex and depends on many factors it is difficult, if not impossible, to determine a combustion parameter which correlates combustion efficiency for all flight and engine operating conditions. However, some of the primary variables affecting combustion efficiency are considered in the combustion parameter  $P_4T_4/V_b$  derived in reference 3. In order to obtain a satisfactory correlation of combustion efficiency with combustion parameter  $P_4T_4/V_b$ , an additional parameter, engine fuel-air ratio, was introduced. Combustion efficiency is presented in figure 17 as a function of these two combustion parameters for two of the compressor-combustor configurations investigated. The data of figure 17(a) were obtained at altitudes from 15,000 to 55,000 feet and flight Mach numbers from 0.17 to 0.99. The data of figure 17(b) represent a range of altitudes from 15,000 to 45,000 feet and flight Mach numbers from 0.17 to 0.62. Although scatter is present, particularly at low values of  $P_4T_4/V_b$ , the curves for several narrow ranges of fuel-air ratio provide a reasonably good correlation of the data. In general, the data in figures 17(a) and 17(b) exhibit about the same magnitudes and trends. In figures 17(a) and 17(b), combustor efficiency begins to decline for values of  $P_4T_4/V_b$  below 34,000 pounds-°R-second per cubic foot. Below this value of  $P_4T_4/V_b$ , combustion efficiency was sensitive to fuel-air ratio, and above this value, fuel-air ratio had a negligible effect.

The data of figure 17 are presented in figure 18 with fuel-air ratio as the abscissa in order to show more clearly the effect of fuel-air ratio on combustion efficiency. Because sufficient data were not available to completely separate the variables,  $P_4T_4/V_b$  and fuel-air ratio, each of the curves presented in figure 18 is for a small range of  $P_4T_4/V_b$ . These data indicate that over these small ranges of  $P_4T_4/V_b$  there was an optimum value of fuel-air ratio for maximum combustion efficiency. For example, for a range of  $P_4T_4/V_b$  of 6500 to 7500 pounds-°R-second per cubic foot, combustion efficiency varied from 0.50 to 0.67 as fuel-air ratio was increased from 0.0066 to 0.0112, and a further increase in fuel-air ratio from 0.0112 to 0.0156 decreased combustion efficiency from 0.675 to 0.55.

Combustion efficiency probably varied with fuel-air ratio at a constant value of combustion parameter because of local rich and lean fuel-air ratio regions in the primary zone of the combustor. These regions may also be influenced by the degree of fuel atomization. At the high values of fuel-air ratio, some of the local regions in the primary zone are probably excessively rich in fuel, and combustion was incomplete because of a lack of oxygen; whereas, at the lower values of fuel-air ratio, some of the local regions were too lean for efficient combustion.

#### Comparison of Several Combustors from Different Turbojet Engines

Performance of four different current combustors is compared in figure 19. Combustion efficiency is shown as a function of combustion parameter  $P_4 T_4 / V_b$  at three different levels of fuel-air ratio.

Combustor A was the combustor used in the prototype J40-WE-8 turbojet engine. Data for combustor M were not available below a combustion parameter of 20,000 pounds-°R-second per cubic foot.

Combustion efficiency of all combustors shown was affected somewhat by fuel-air ratio, probably because of the rich and lean combustion regions previously discussed. This effect of fuel-air ratio was greatest at low values of combustion parameter  $P_4 T_4 / V_b$ .

For the range of combustor operating conditions investigated, the performance of combustors A, M, and N was approximately the same. These combustors have fuel systems that provide good fuel atomization and distribution over a wide range of fuel flows. Combustor P had a lower combustion efficiency than combustors A, M, and N, especially at low values of combustion parameter and fuel-air ratio. The low combustion efficiencies experienced with combustor P are felt to be primarily a result of the fixed-area fuel nozzles which provide poor spray and penetration characteristics at low fuel flows. Of course, combustion efficiency is primarily a function of matching the fuel and air properly and not of fuel injection alone; nevertheless, for the combustors presented, combustion efficiency is concluded to be primarily dependent on the method of fuel injection rather than the type of combustor used.

#### SUMMARY OF RESULTS

1. The effect of combustor hole-area distribution and combustor inlet-air pressure profile on combustor performance was obtained over a range of engine speeds at an altitude of 30,000 feet and a flight Mach number of 0.62:

(a) The combustors with a lower percentage of total hole area at the inner wall had a higher combustor-outlet temperature profile near the inner wall than the combustor with equal hole-area distribution; the converse was true near the outer wall. As the combustor inlet-air pressure profile was lowered (corresponding to a reduction in air flow) at the inner portion of the passage height, the combustor-outlet temperature profile near the inner wall was raised. Similar trends were encountered near the outer wall.

(b) Combustor pressure-loss coefficient was not affected by hole-area distribution but was affected by total hole area and inlet-air pressure profile. For combustors with total hole area of 877 and 809 square inches, the pressure-loss coefficient was 10.8 and 12.4, respectively, at a combustor density ratio of 2.2. For changes in inlet-air pressure profile, the pressure-loss coefficient varied from 10.8 to 15.8 at a density ratio of 2.2. There was no discernible effect of these variables on combustion efficiency.

2. With compressor 1 and combustor A, which was the configuration designated the prototype J40-WE-8, data were obtained over a range of altitudes from 15,000 to 55,000 feet and flight Mach numbers from 0.17 to 0.99.

(a) These data showed that, in general, a change in corrected engine speed, altitude, flight Mach number or exhaust-nozzle area in order to increase the combustor-inlet pressure resulted in an increase in combustion efficiency except at high pressure levels where combustion efficiency was constant. For example, at a flight Mach number of 0.62 and an open exhaust nozzle (area, 534 sq in.) the combustion efficiency decreased from 0.98 to 0.83 as altitude was increased from 15,000 to 55,000 feet at a corrected engine speed of 7600 rpm.

(b) For all flight conditions and exhaust-nozzle areas, combustor total-pressure-loss ratio decreased as the corrected engine speed increased above a corrected engine speed of about 6000 rpm. However, at a constant corrected engine speed, decreasing altitude, or increasing flight Mach number or exhaust-nozzle area, in general, resulted in an increasing total-pressure-loss ratio. At a corrected engine speed of 7000 rpm, an altitude of 35,000 feet, and a flight Mach number of 0.62, an increase in the exhaust-nozzle area from 367 to 534 square inches resulted in an increase of combustor total-pressure-loss ratio from 0.024 to 0.036.

3. A good correlation was obtained when combustion efficiency was presented as a function of combustion parameter  $P_4 T_4 / V_b$  and engine fuel-air ratio. These data indicated that at values of combustion

parameter below 34,000 pounds-per-second per cubic foot there was a fuel-air ratio that resulted in an optimum combustion efficiency for a given value of combustion parameter.

Lewis Flight Propulsion Laboratory  
National Advisory Committee for Aeronautics  
Cleveland, Ohio

2626

## APPENDIX A

## SYMBOLS

The following symbols are used in this report:

A	cross-sectional area, sq ft
$c_p$	specific heat at constant pressure, Btu/(lb)(°F)
$c_v$	specific heat at constant volume, Btu/(lb)(°F)
f/a	fuel-air ratio
g	acceleration due to gravity, 32.2 ft/sec <sup>2</sup>
H	enthalpy
M	Mach number
N	engine speed, rpm
P	total pressure, lb/sq ft abs
p	static pressure, lb/sq ft abs
q	theoretical dynamic pressure, lb/sq ft abs
R	gas constant, 53.4 ft-lb/(lb)(°R)
T	total temperature, °R
t	static temperature, °R
V	velocity, ft/sec
$W_a$	air flow, lb/sec
$W_f$	fuel flow, lb/hr
$W_g$	gas flow, lb/sec
$\gamma$	ratio of specific heats, $c_p/c_v$
$\delta$	pressure correction factor, $P/2116$ (total pressure divided by NACA standard sea-level pressure)

- 2626
- $\eta$  efficiency
- $\theta$  temperature correction factor,  $\gamma T / (1.4)(519)$  (product of  $\gamma$  and total temperature divided by product of  $\gamma$  at standard sea-level temperature and standard NACA sea-level temperature)
- $\rho$  density,  $(\text{lb})(\text{sec}^2)/\text{ft}^4$

## Subscripts:

- 0 free-stream conditions
- 1 cowl inlet
- 3 compressor inlet
- 4 combustor inlet, compressor outlet
- 5 combustor outlet, turbine inlet
- 6 turbine outlet
- 7 exhaust-nozzle outlet
- b burner
- c compressor
- i indicated
- t turbine
-

## APPENDIX B

## METHODS OF CALCULATION

Air flow. - Air flow was calculated at station 1 (fig. 2) by use of the following equation

$$W_{a,1} = p_1 A_1 \sqrt{\frac{2\gamma_1 g}{(\gamma_1 - 1) R t_1} \left[ \left( \frac{p_1}{p_1} \right)^{\frac{\gamma_1 - 1}{\gamma_1}} - 1 \right]}$$

Gas flow downstream of the combustor is

$$W_g = W_{a,1} + \frac{W_f}{3600}$$

Combustor dynamic pressure. - In order to calculate a combustor dynamic pressure, based on a combustor maximum cross-sectional area of 6.40 square feet, a combustor Mach number was first calculated with the equation

$$\frac{M_b}{\left( 1 + \frac{\gamma_4 - 1}{2} M_b^2 \right)^{\frac{\gamma_4 + 1}{2(\gamma_4 - 1)}}} = \frac{W_{a,4} \sqrt{T_4}}{0.776 A_b P_4 \sqrt{\gamma_4}}$$

then

$$q_b = \frac{\gamma_4 P_4 M_b^2}{2}$$

and

$$P_4 = \frac{P_4}{\left( 1 + \frac{\gamma_4 - 1}{2} M_b^2 \right)^{\frac{\gamma_4}{\gamma_4 - 1}}}$$

therefore

$$q_b = \frac{\gamma_4 P_4 M_b^2}{2 \left( 1 + \frac{\gamma_4 - 1}{2} M_b^2 \right)^{\frac{\gamma_4}{\gamma_4 - 1}}}$$

Combustor-inlet velocity. - With the use of combustor Mach number  $M_b$ , combustor-inlet velocity was determined from the following equation:

$$V_b = M_b \sqrt{\gamma_4 g R t_4}$$

where

$$t_4 = \frac{T_4}{\left(1 + \frac{\gamma_4 - 1}{2} M_b^2\right)}$$

Turbine-inlet temperature. - Turbine-inlet temperature was calculated from the following equation, which assumes compressor and turbine work equal:

$$T_5 = \frac{W_{a,1} c_{p,c}}{W_{g,5} c_{p,t}} (T_4 - T_1) + T_7$$

Combustion efficiency. - With the assumption that the compressor and turbine work are equal, combustion efficiency is defined as the ratio of the actual enthalpy rise of the gas while passing through the engine to the theoretical increase in enthalpy that would result from complete combustion of the fuel charge.

$$\eta_b = \frac{\text{actual enthalpy rise of the gas across the engine}}{\text{heat input}}$$

$$= \frac{3600 \left[ W_{a,1} H_a \right]_{T_1}^{T_7} + \left[ W_f H_f \right]_{T_b}^{T_7}}{18,700 W_f}$$

where 18,700 Btu per pound of fuel is the lower heating value of the fuel.

Combustor total-density ratio. - From the gas law the total density is

$$\rho = \frac{P}{gRT}$$

then

$$\frac{\rho_4}{\rho_5} = \frac{P_4}{P_5} \frac{T_5}{T_4}$$

## REFERENCES

1. Finger, Harold B., Essig, Robert H., and Conrad, E. William: Effect of Rotor- and Stator-Blade Modifications on Surge Performance of an 11-Stage Axial-Flow Compressor. I - Original Production Compressor of XJ40-WE-6 Engine. NACA E52G03, 1952
2. Conrad, E. William, Finger, Harold B., and Essig, Robert H.: Effect of Rotor- and Stator-Blade Modification on Surge Performance of an 11-Stage Axial-Flow Compressor. II - Redesigned Compressor for XJ40-WE-6 Engine. NACA RM E52I10, 1953.
3. Childs, J. Howard: Preliminary Correlation of Efficiency of Aircraft Gas-Turbine Combustors for Different Operating Conditions. NACA RM E50F15, 1950.
4. Pinkel, I. Irving, and Shames, Harold: Analysis of Jet-Propulsion-Engine Combustion-Chamber Pressure Losses. NACA Rep. 880, 1947. (Supersedes NACA TN 1180.)















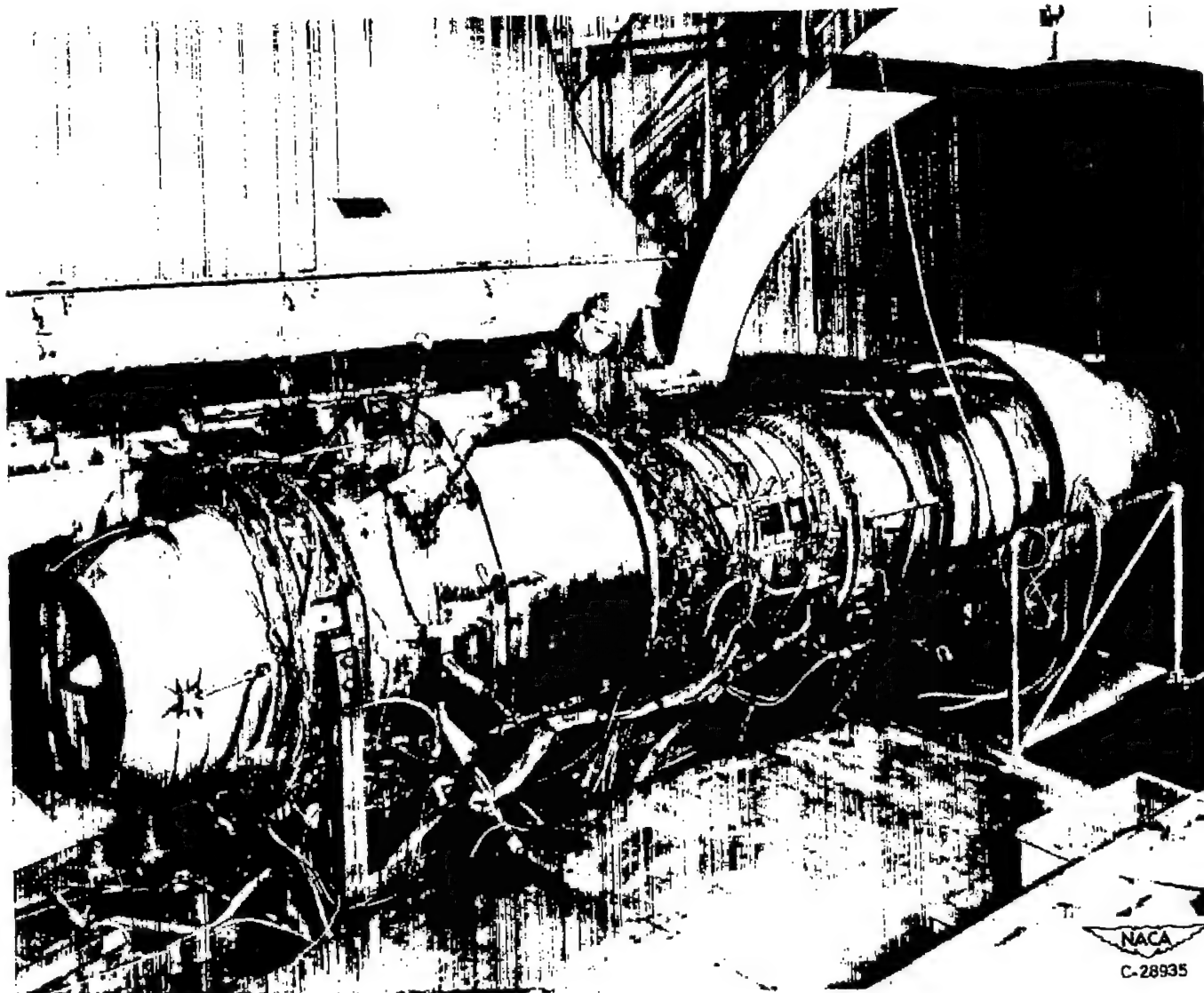
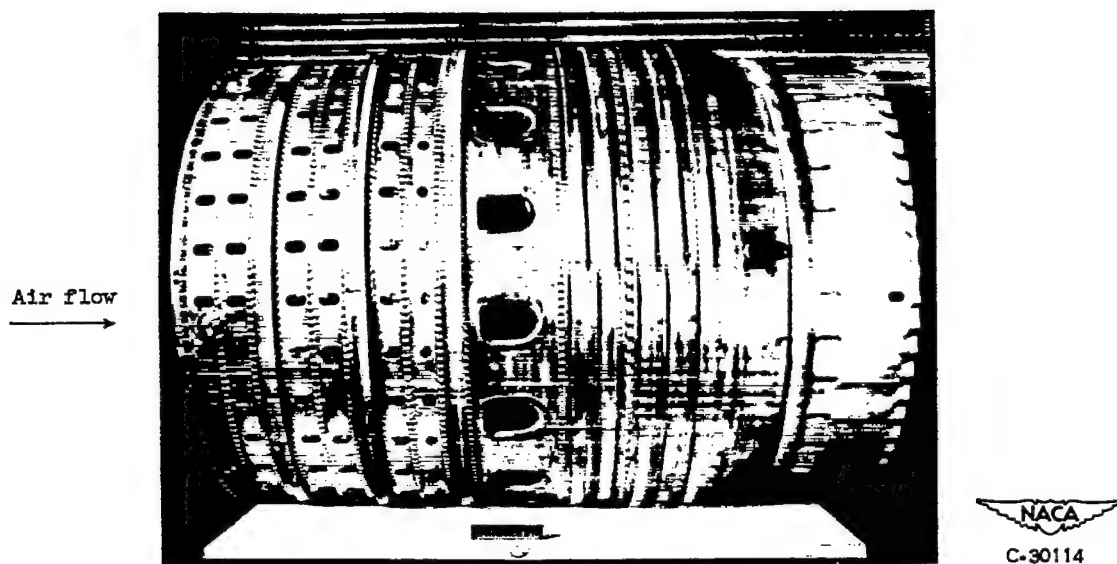
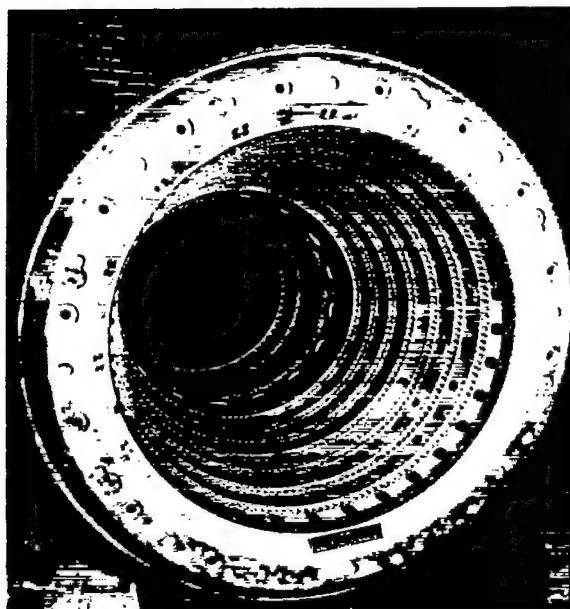


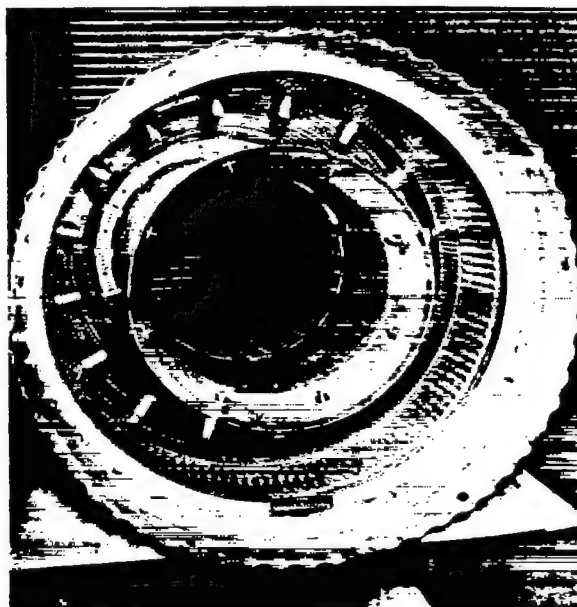
Figure 1 - Engine installation in altitude wind tunnel test section.



(a) Side view.



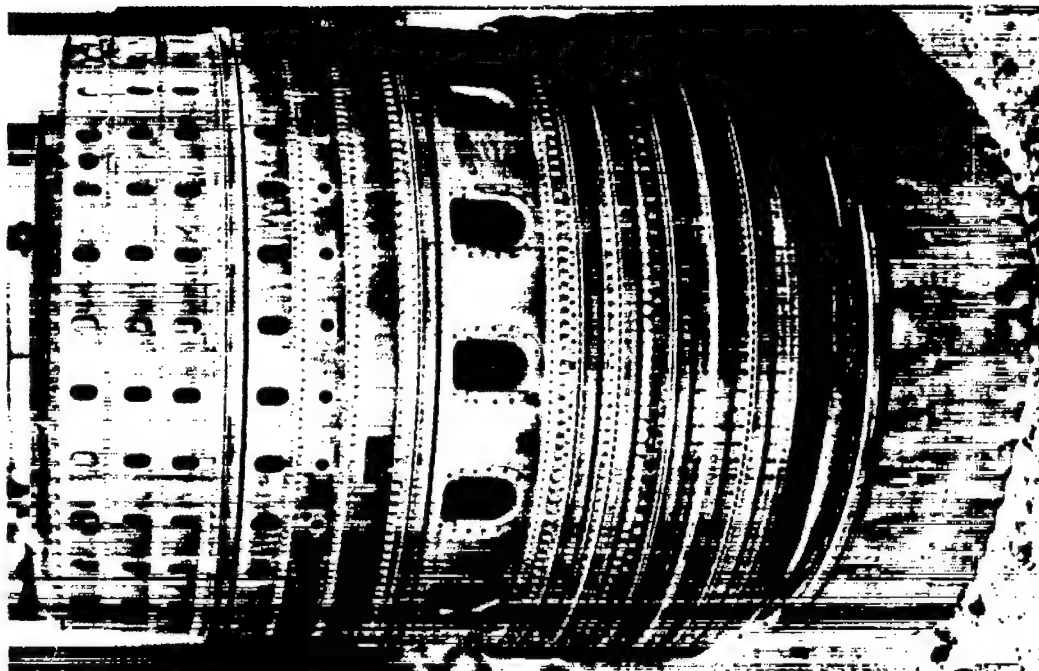
(b) Front view.



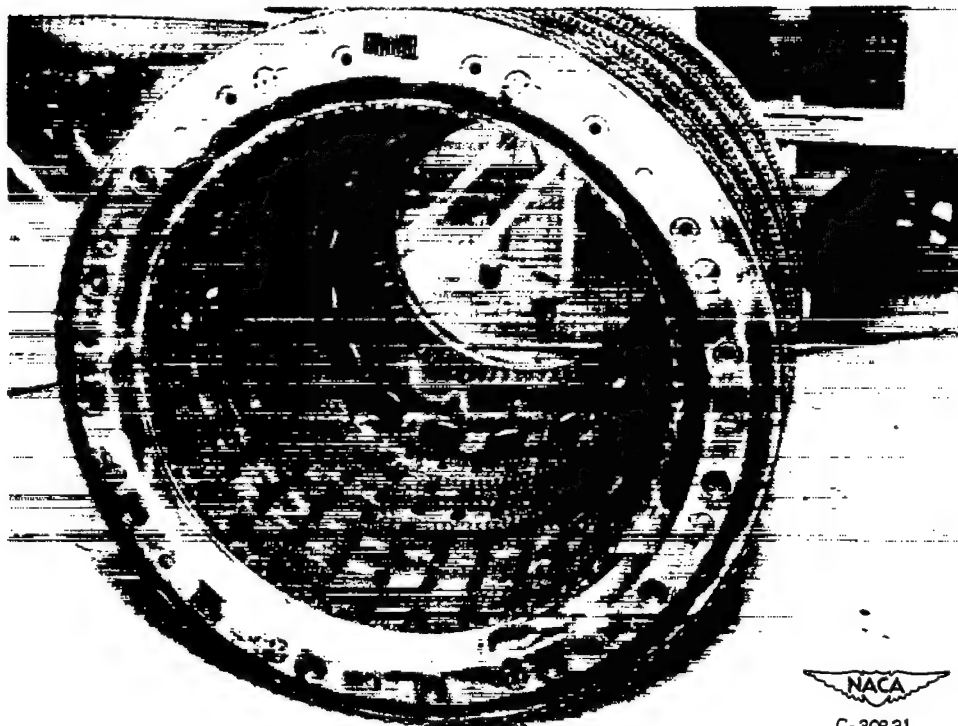
(c) Rear view.

Figure 2. - Engine combustor A.

Air  
flow  
→



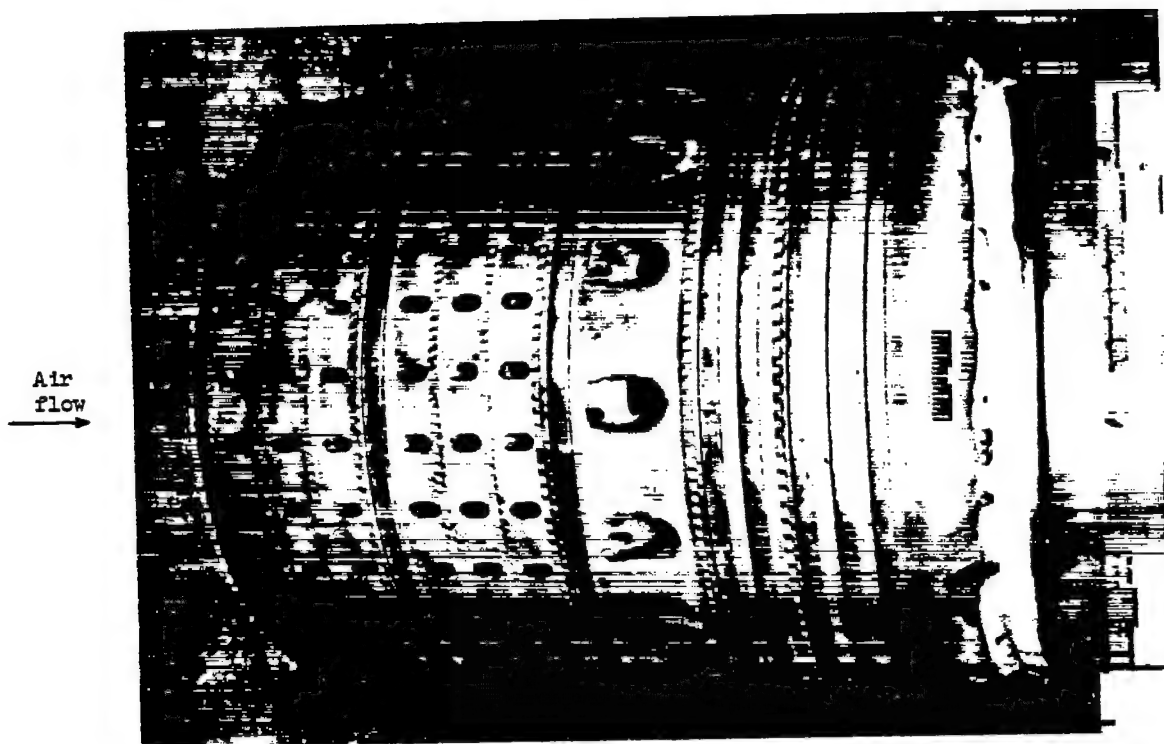
(a) Side view.



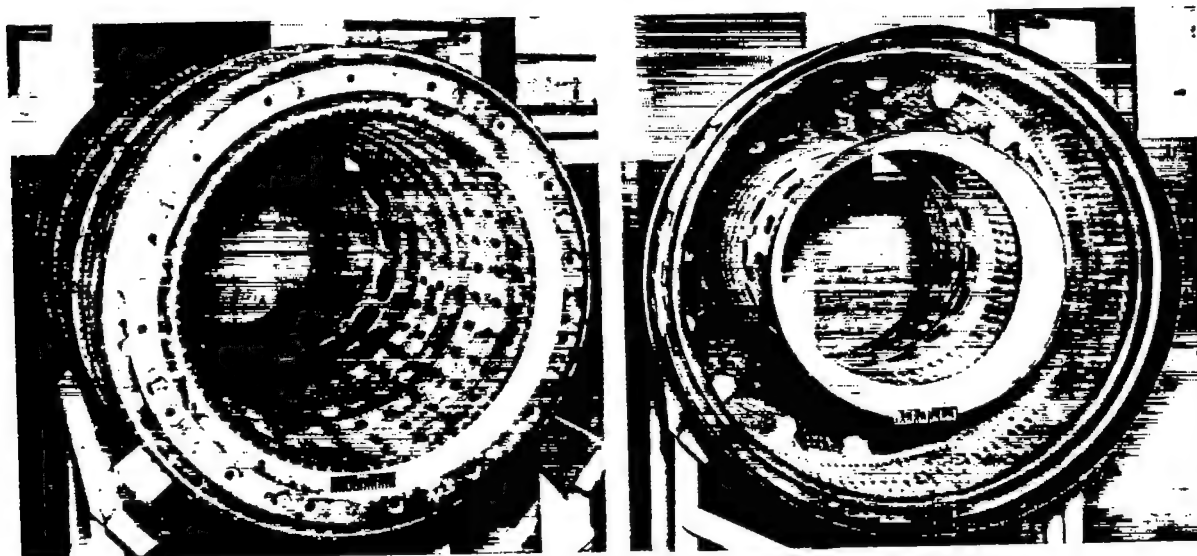
(b) Front view.

Figure 3. - Engine combustor B.

NACA  
C-30831



(a) Side view.



(b) Front view.

(c) Rear view.

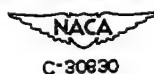


Figure 4. - Engine combustor C.

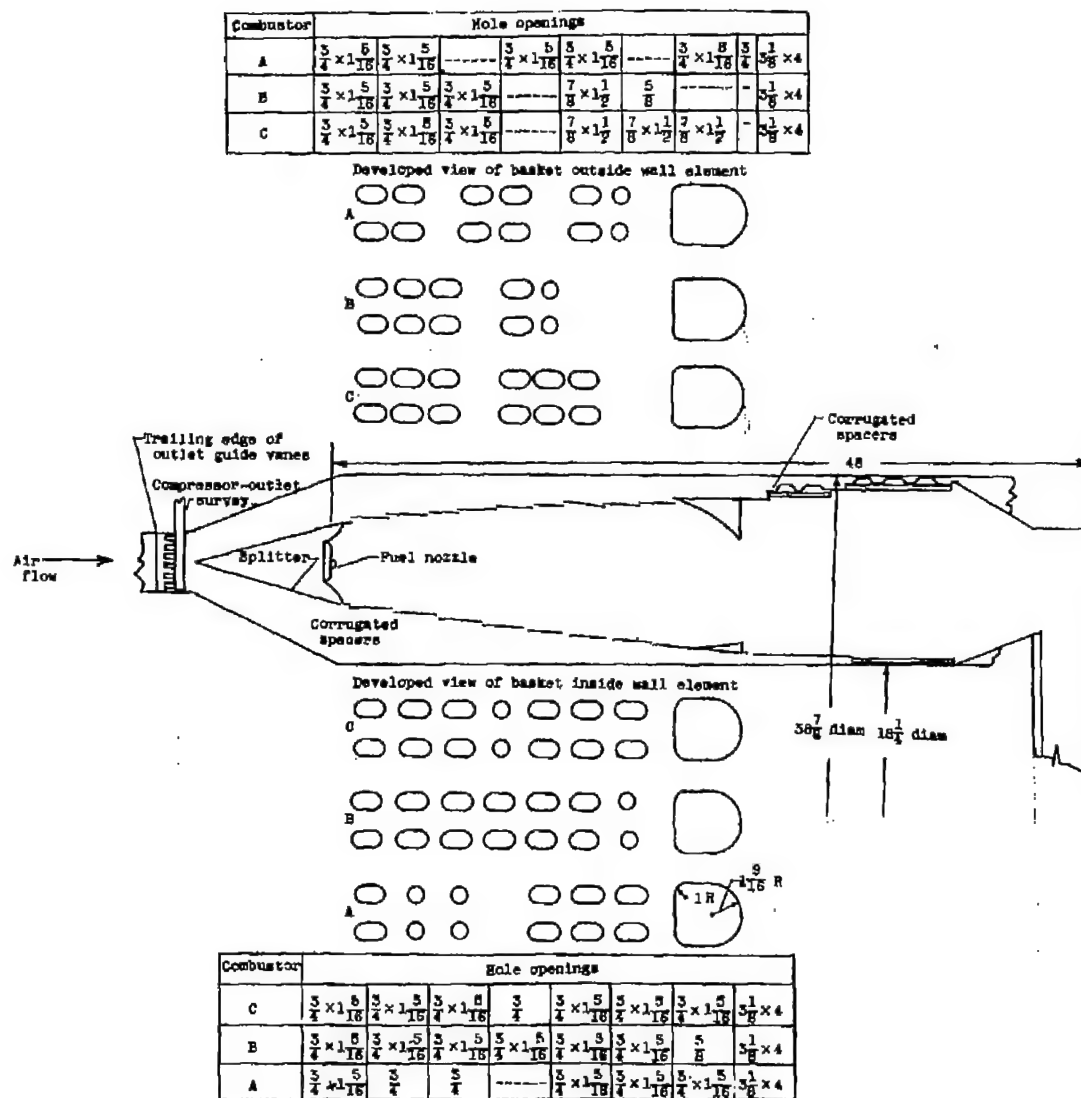


Figure 5. - Combustor-basket configurations. All dimensions are in inches.

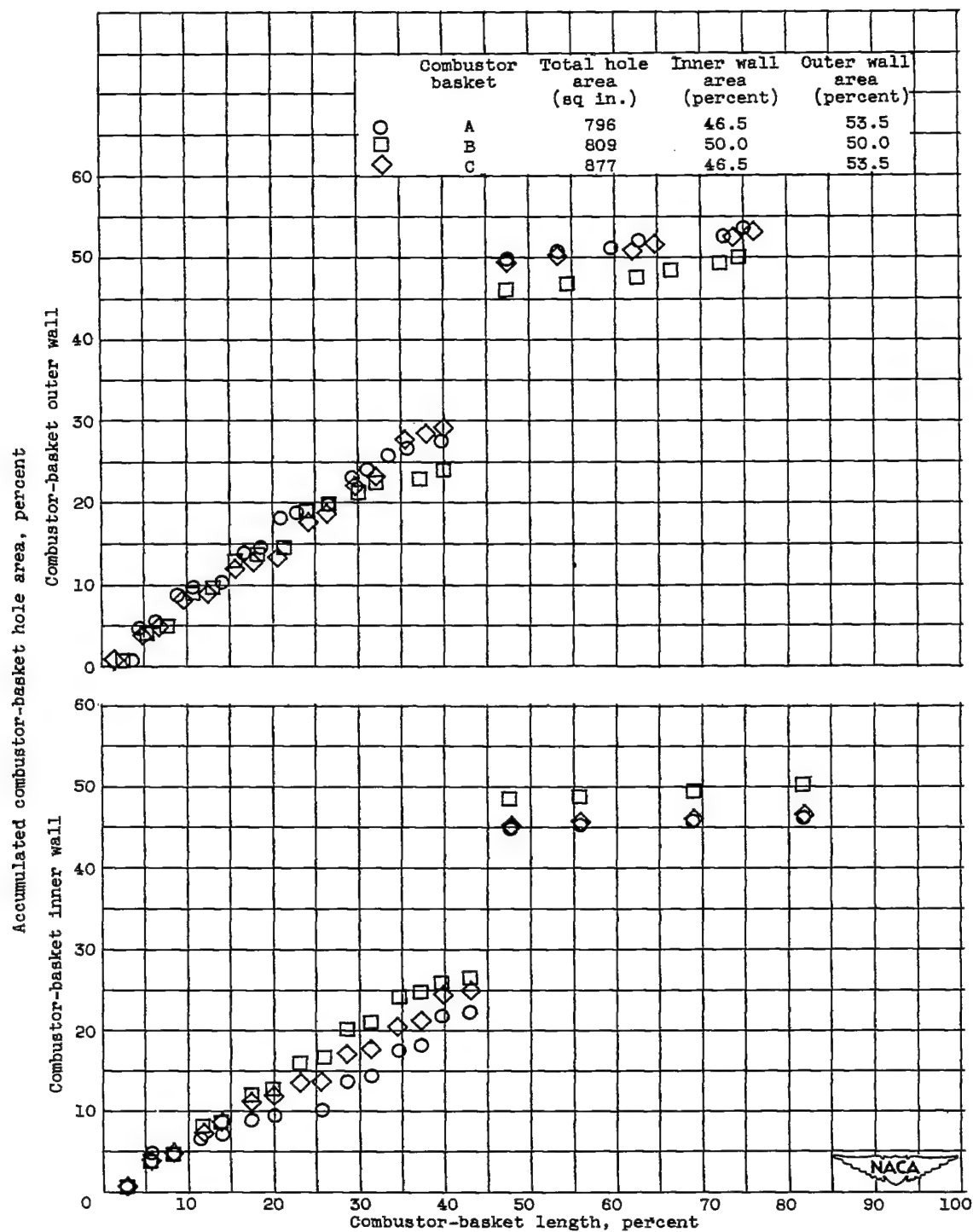
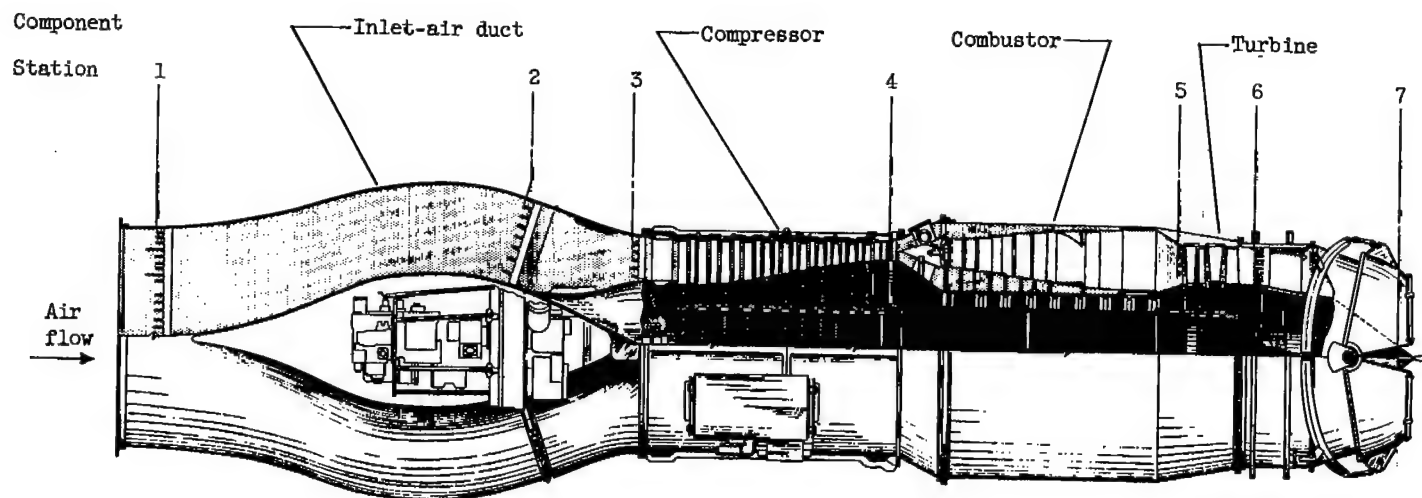


Figure 6. - Percentage of total open area of combustor baskets.



NACA  
CD-2732

Station	Location	Total-pressure tubes	Static-pressure tubes	Wall static-pressure orifices	Thermo-couples
1	Inlet-air duct	29	12	6	10
2	Engine inlet	18	0	4	0
3	Compressor inlet	23	3	7	0
4	Compressor outlet	18	0	3	6
5	Turbine inlet	5	0	0	10*
6	Turbine outlet	20	0	8	24
7	Exhaust-nozzle outlet	16	2	8	0

\*Sonic flow probes

Figure 7. - Top view of turbojet-engine installation showing stations at which instrumentation was installed.

2626

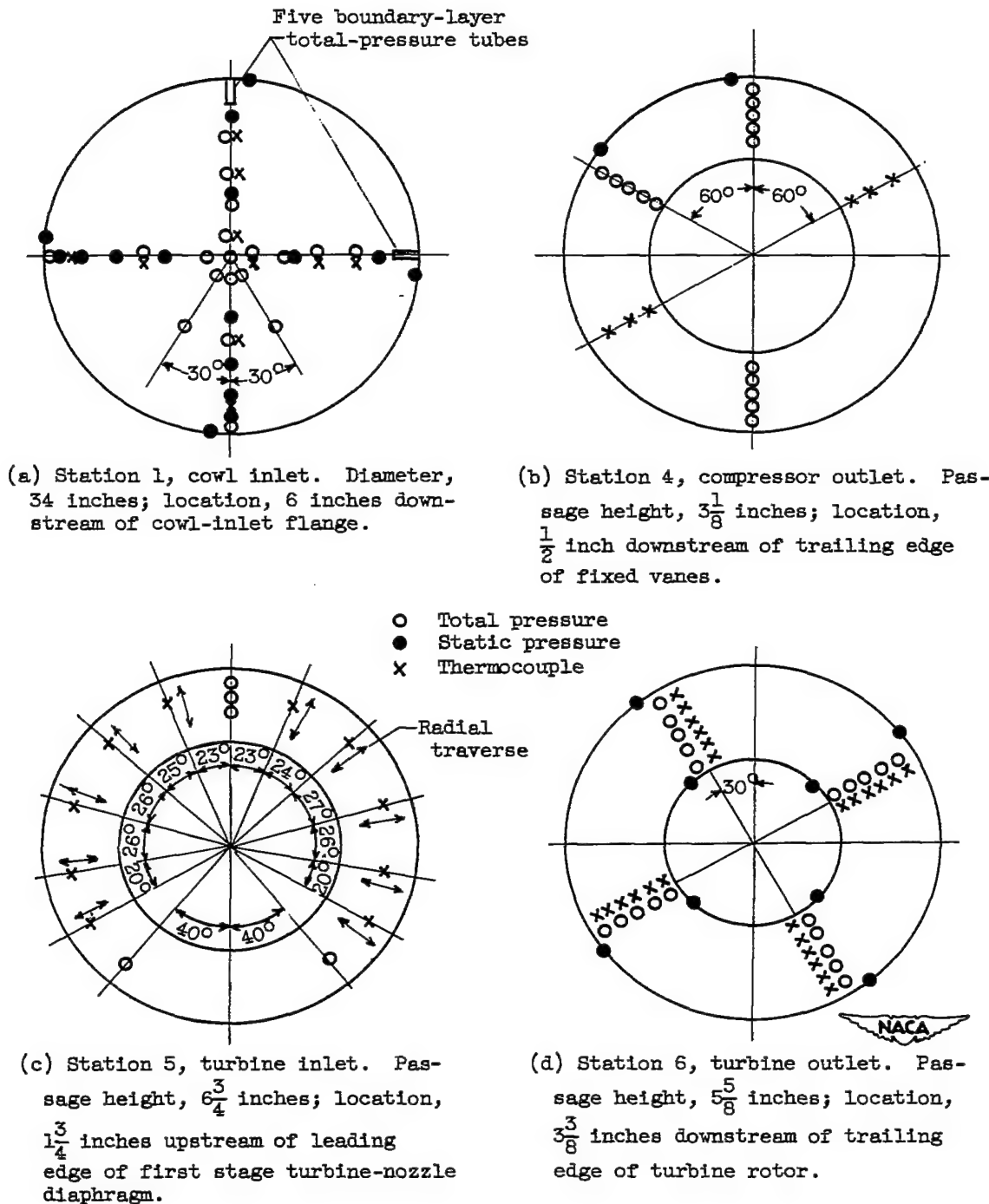


Figure 8. - Location of instrumentation. Viewed looking downstream.

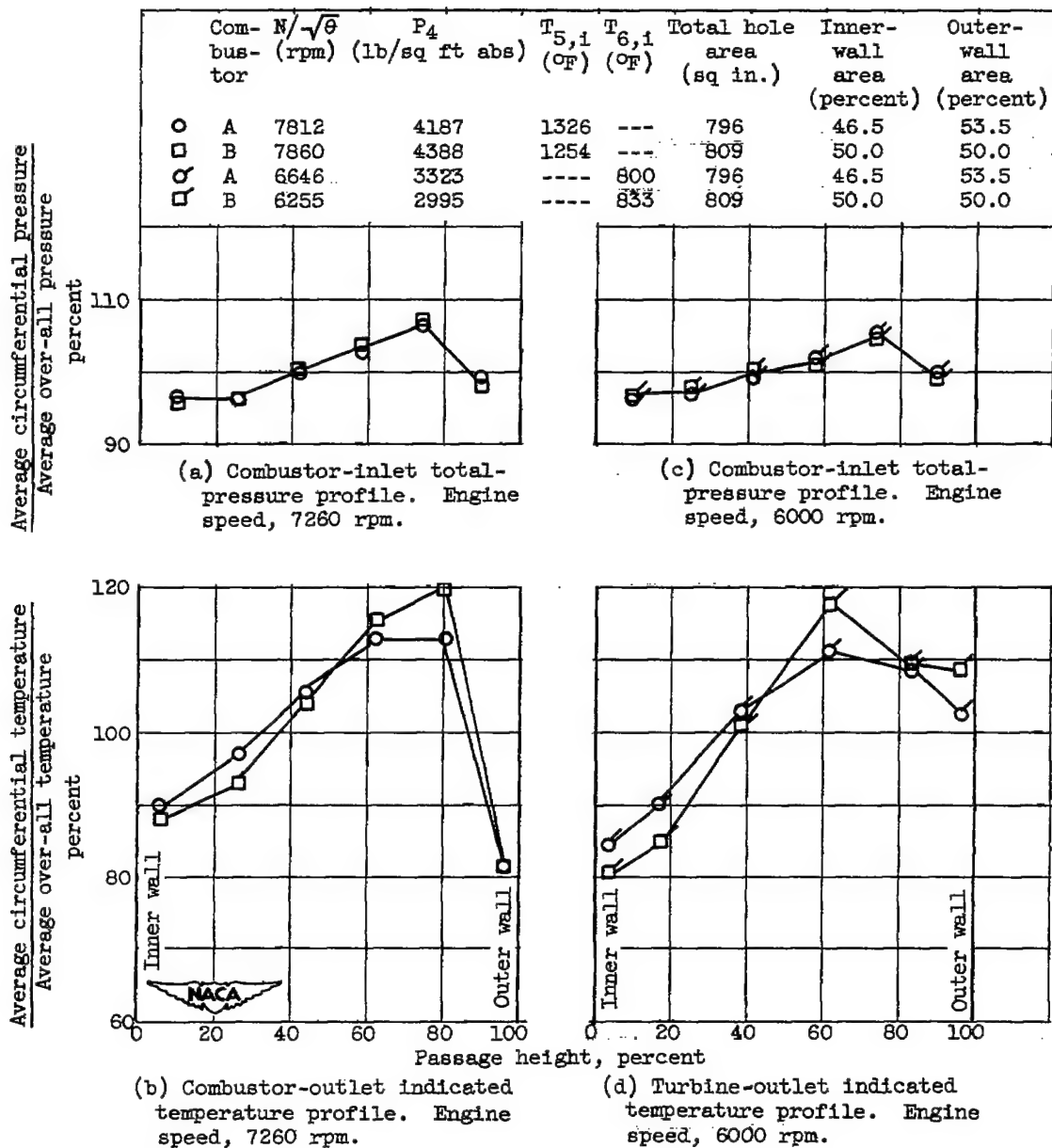


Figure 9. - Effect of combustors on combustor-outlet indicated temperature profiles. Altitude, 30,000 feet; flight Mach number, 0.62; compressor, 1.

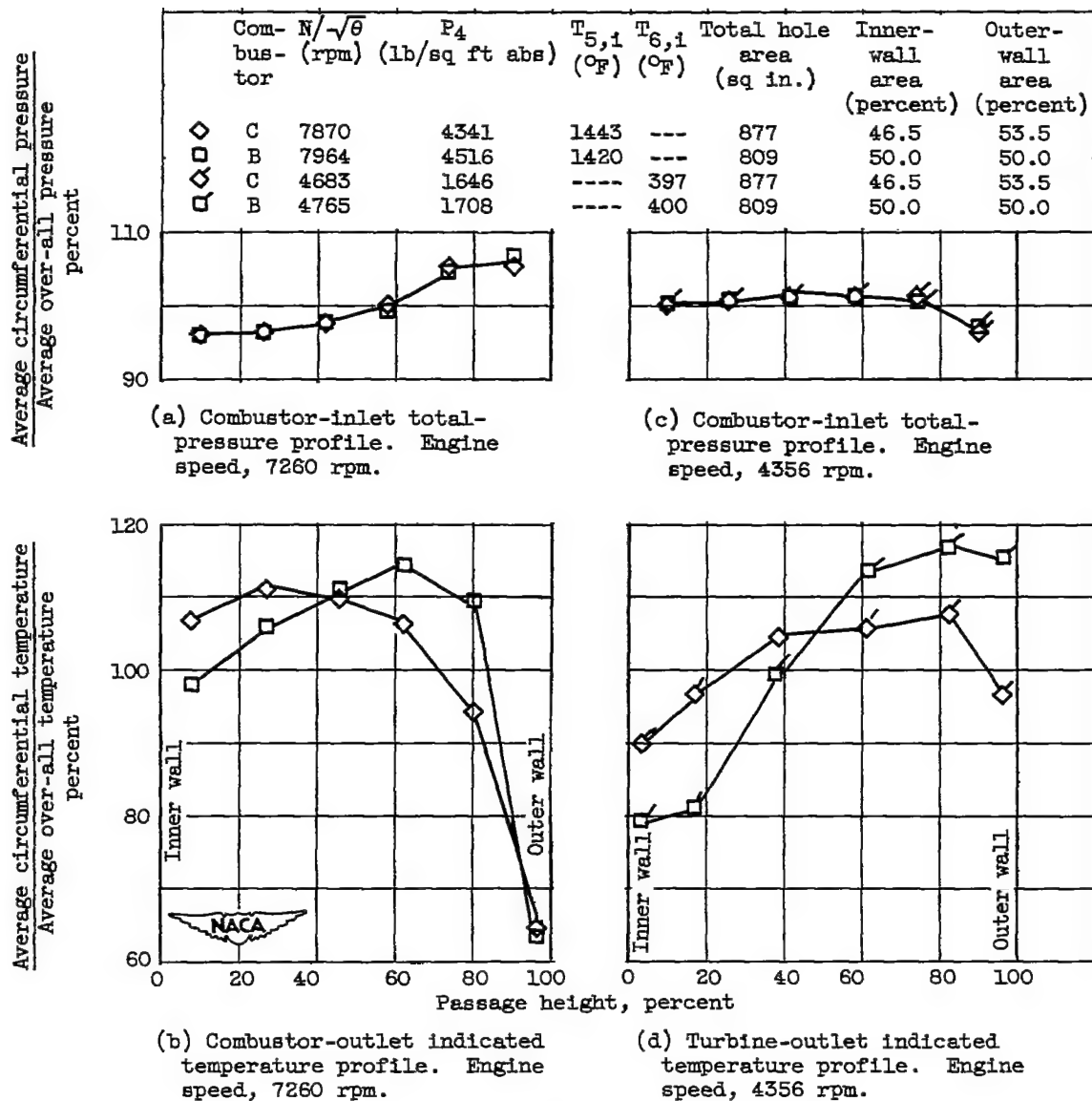


Figure 10. - Effect of combustors on combustor-outlet indicated temperature profiles. Altitude, 30,000 feet; flight Mach number, 0.62; compressor, 3.

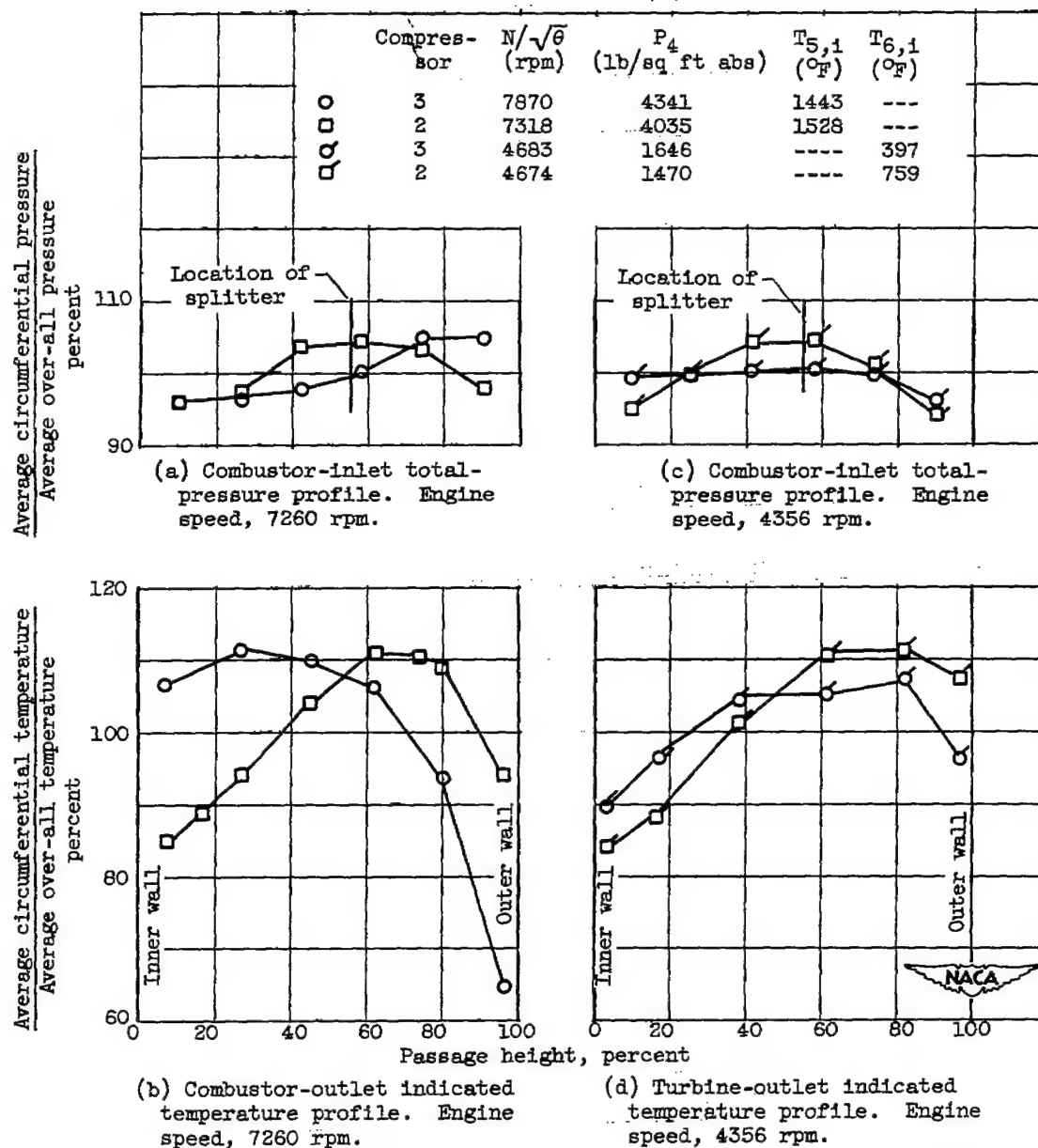


Figure 11. - Effect of combustor inlet-air pressure profiles on combustor-outlet indicated temperature profiles. Altitude, 30,000 feet; flight Mach number, 0.62; combustor, C.

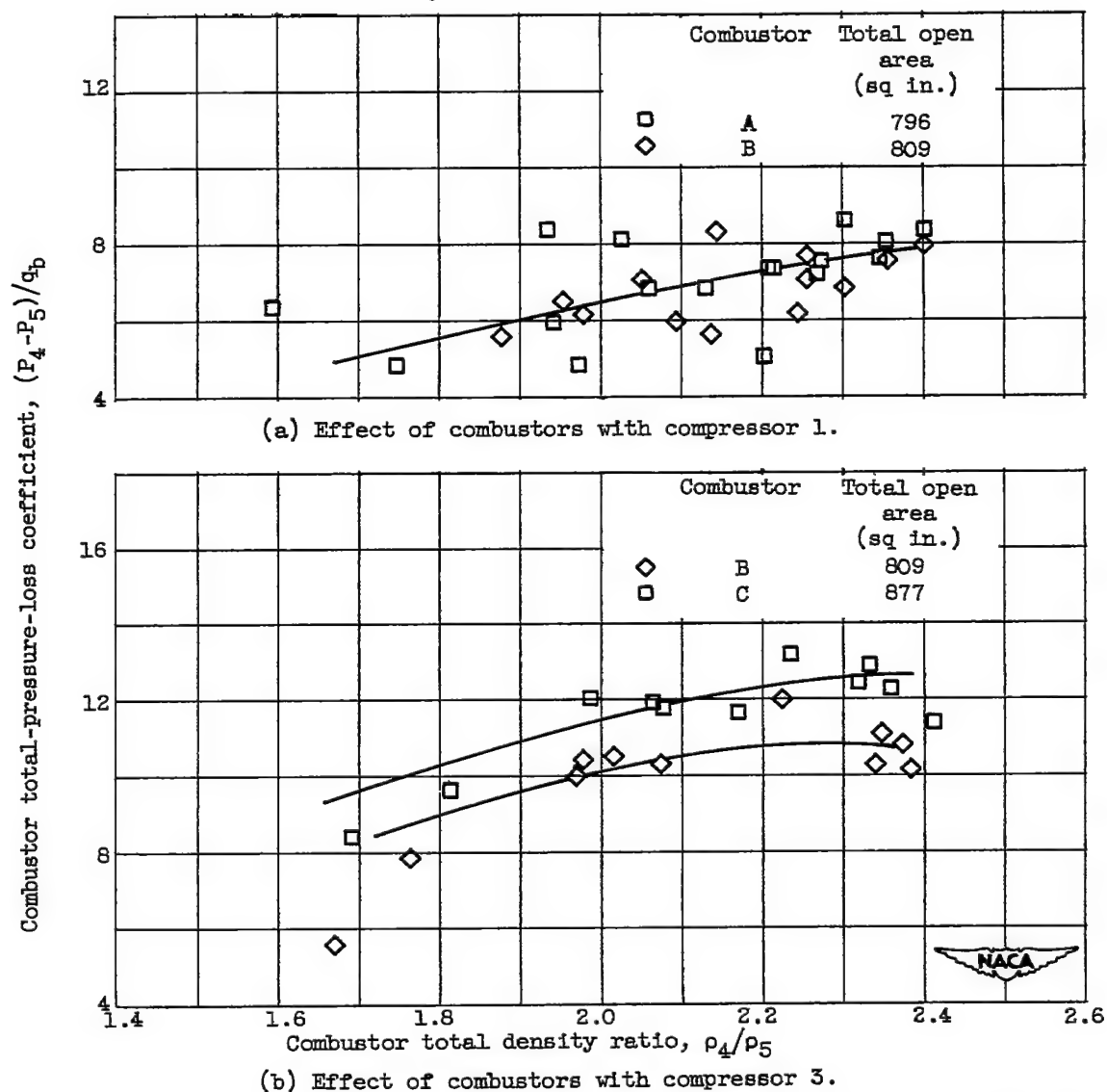
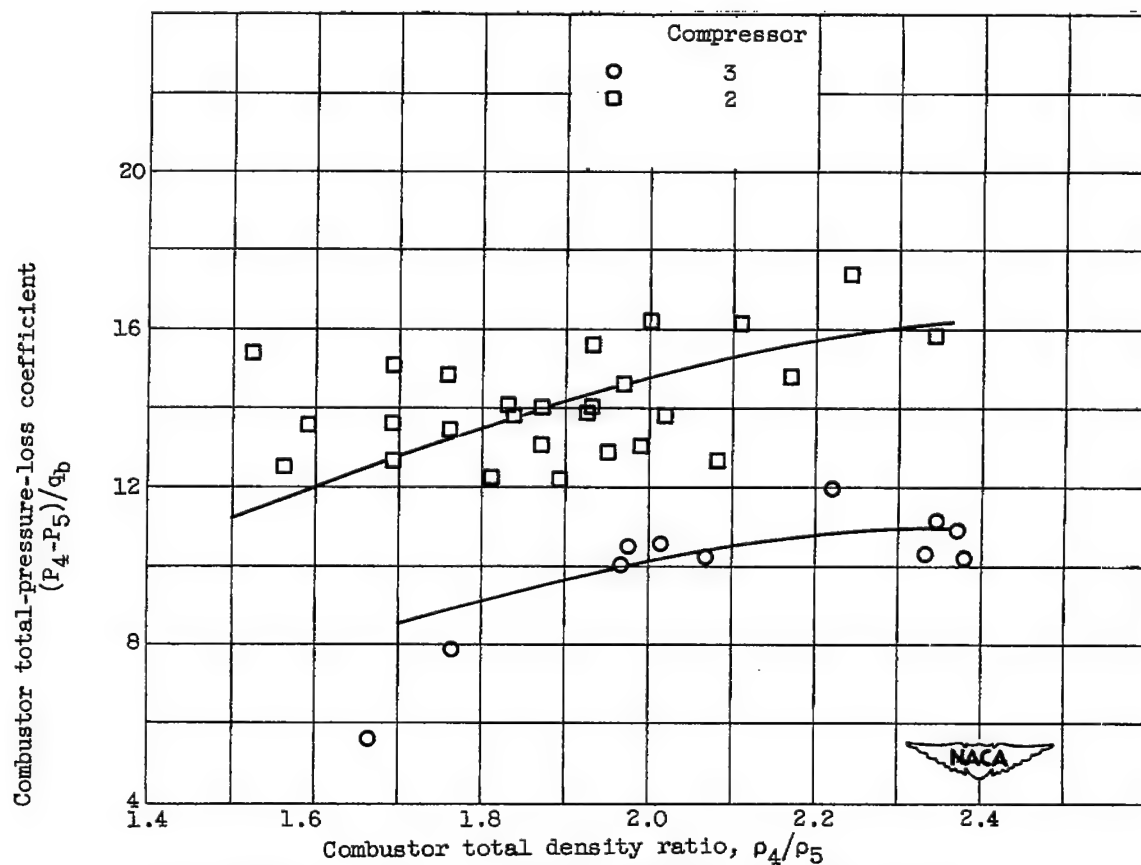


Figure 12. - Variation of combustor total-pressure-loss coefficient with density ratio for several combustors. Altitude, 30,000 feet; flight Mach number, 0.62.



(c) Effect of inlet-air pressure profiles with combustor C.

Figure 12. - Concluded. Variation of combustor total-pressure coefficient with density ratio for several combustors. Altitude, 30,000 feet; flight Mach number, 0.62.

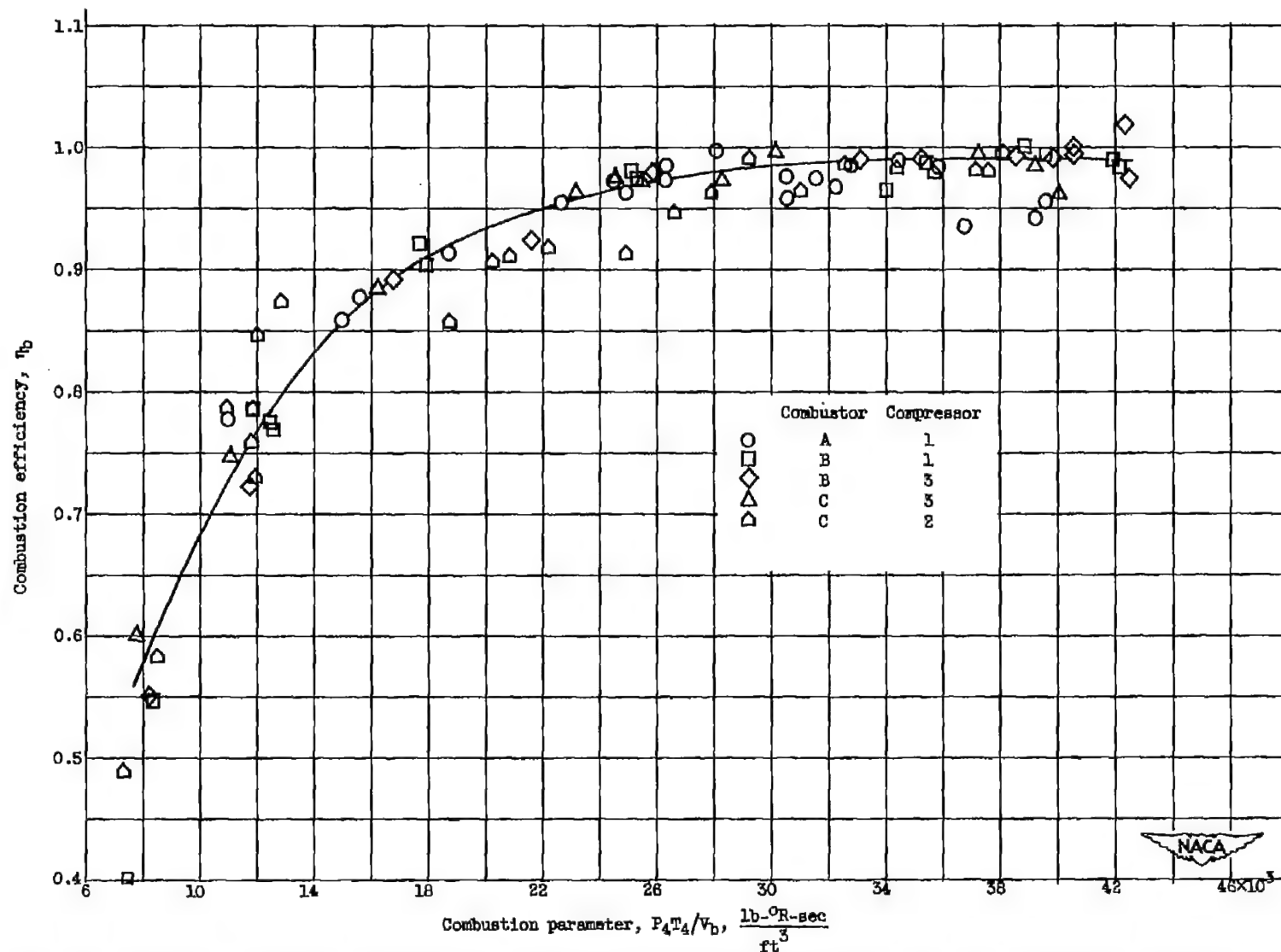


Figure 13. - Variation of combustion efficiency with combustion parameter for three combustors and three compressors. Altitude, 30,000 feet; flight Mach number, 0.62.

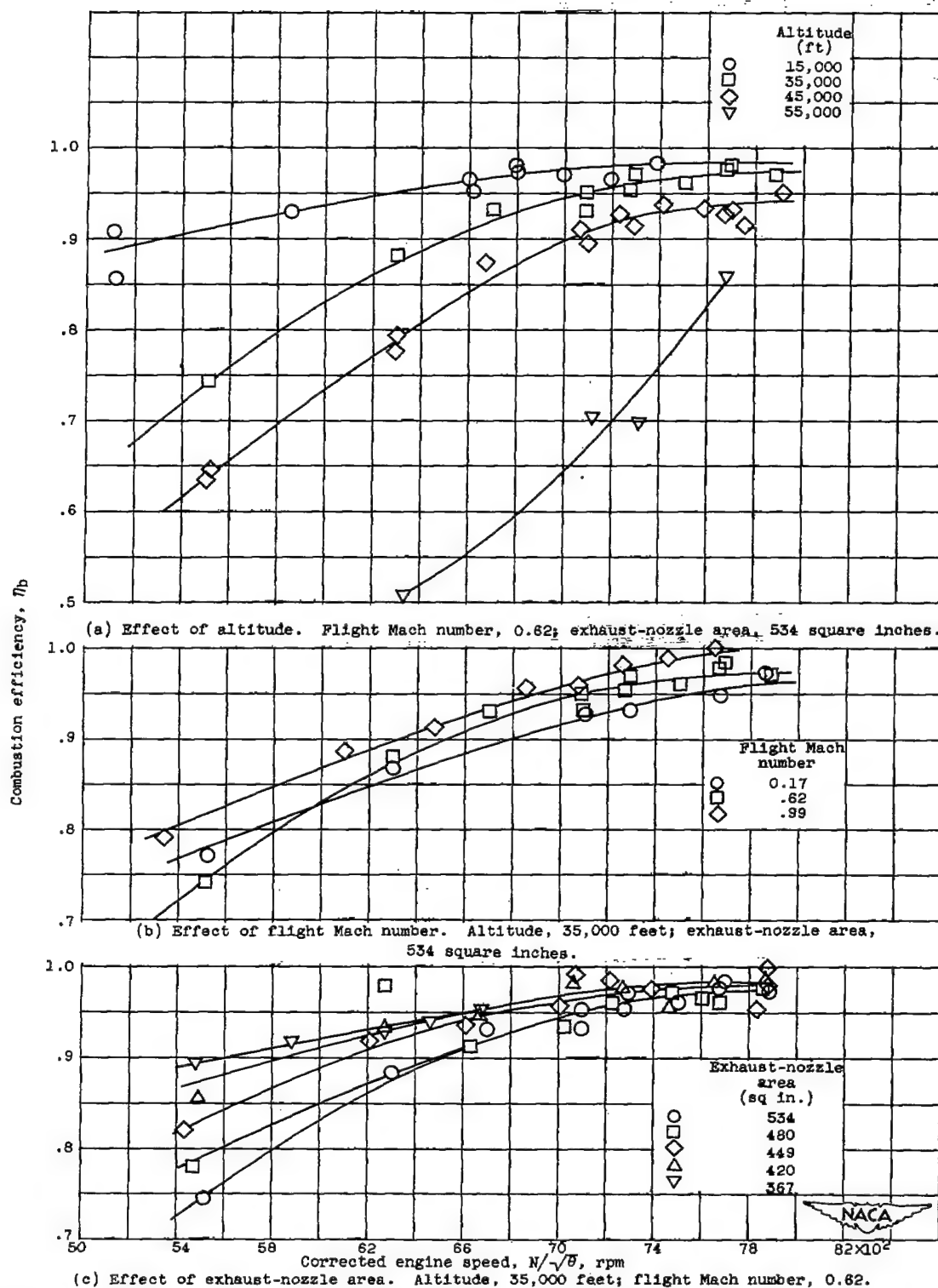


Figure 14. - Variation of combustion efficiency with corrected engine speed. Prototype J40-WE-8 turbojet engine (compressor 1, combustor A).

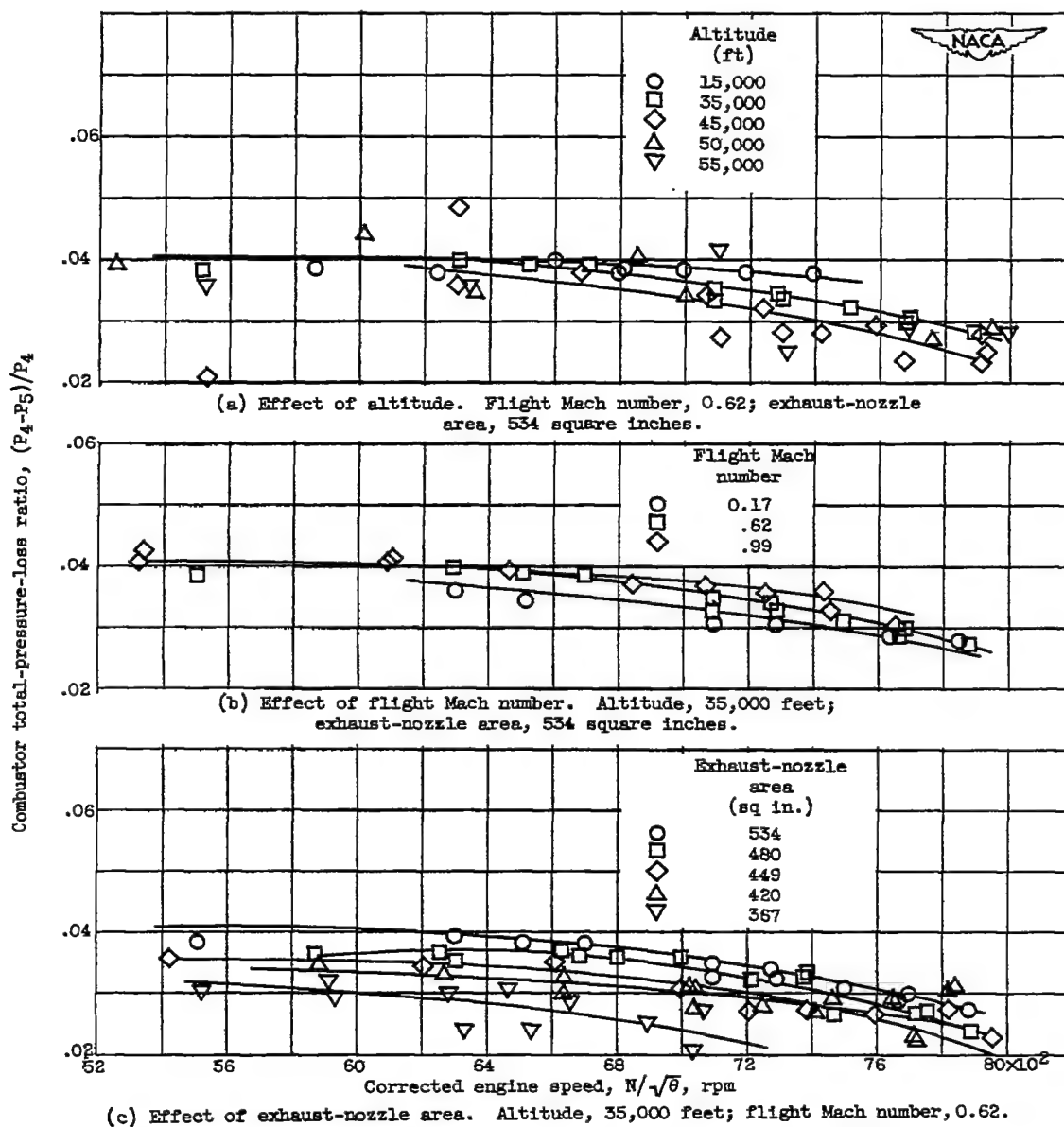


Figure 15. - Combustor pressure-loss characteristics in terms of engine parameters. Prototype J40-WE-8 turbojet engine (compressor 1, combustor A).

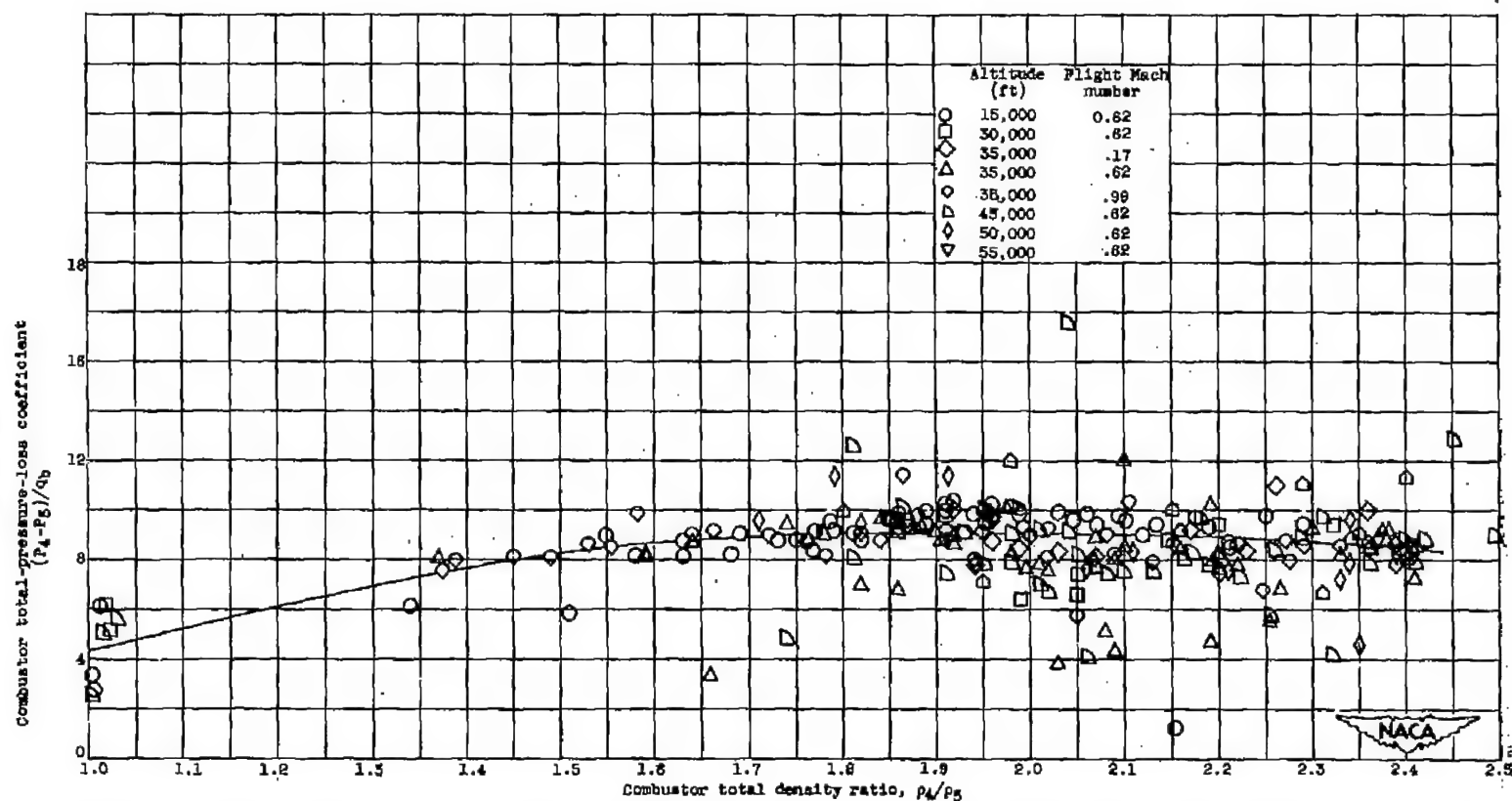
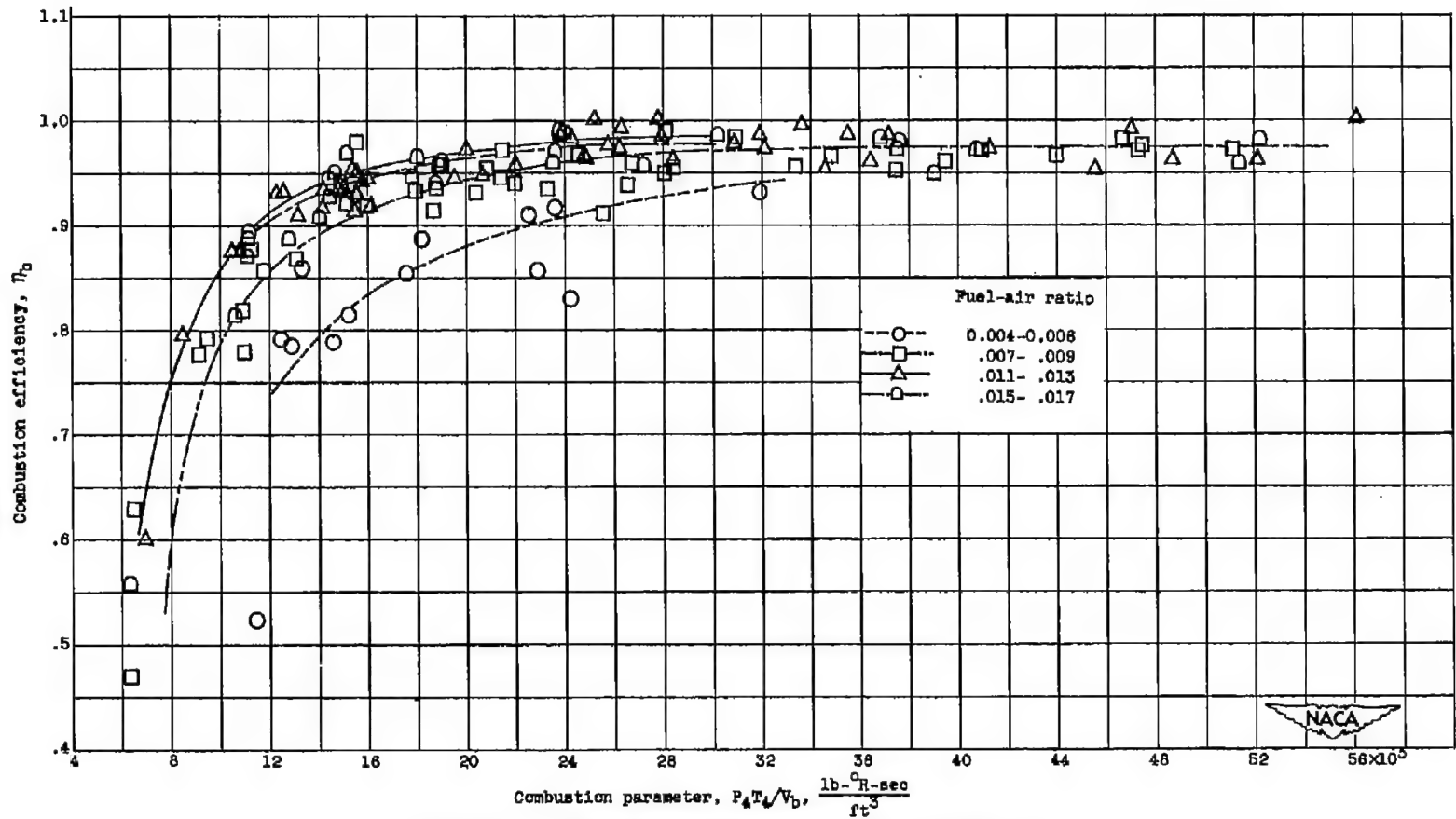
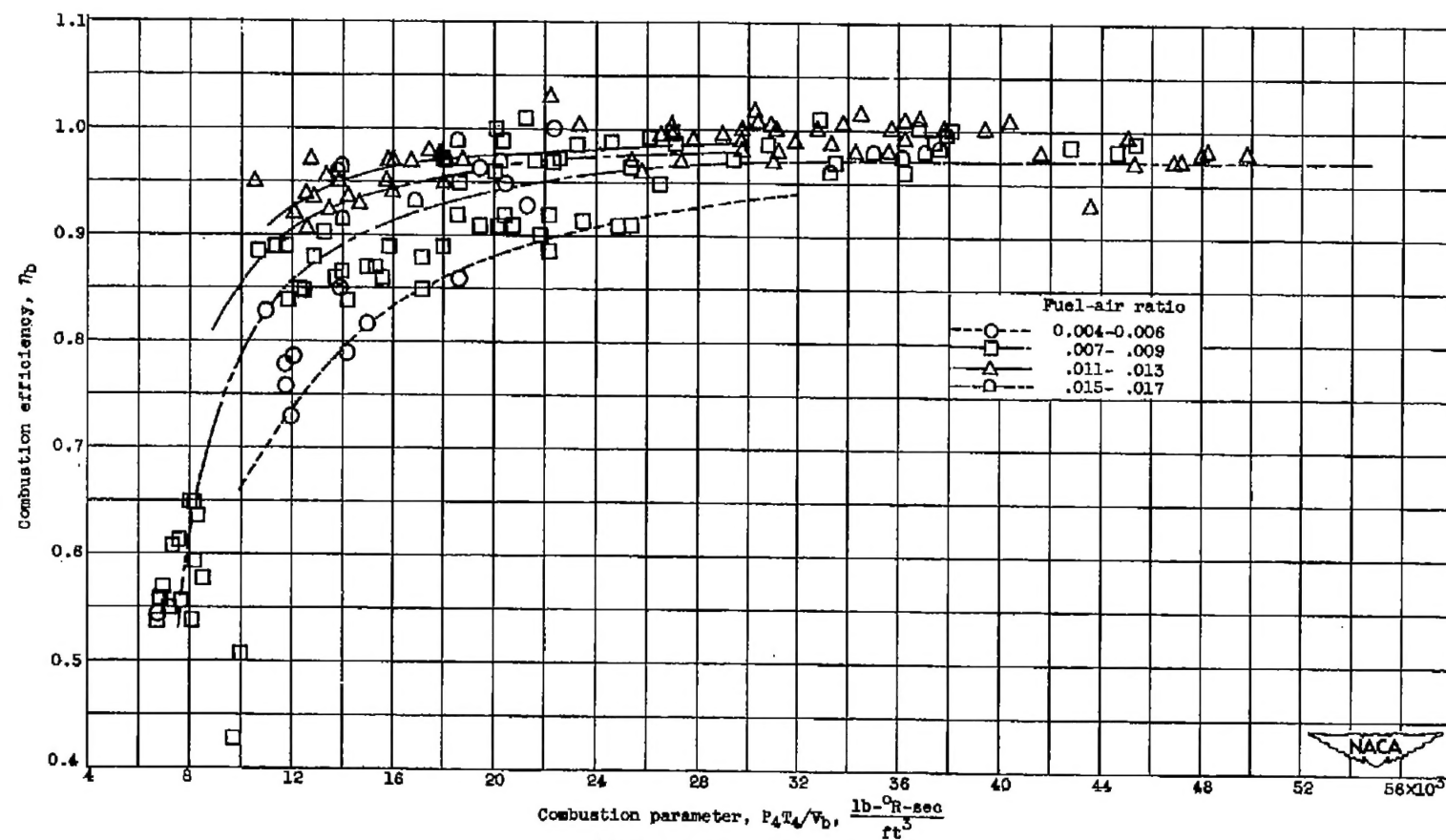


Figure 18. - Combustor pressure-loss characteristics in terms of combustor parameters. Prototype J40-W2-8 turbojet engine (compressor 1, combustor A).



(a) Prototype J40-WE-8 turbojet engine (compressor 1, combustor A).  
Figure 17. - Variation of combustion efficiency with combustion parameter.



(b) Compressor 2, combustor C.

Figure 17. - Concluded. Variation of combustion efficiency with combustion parameter.

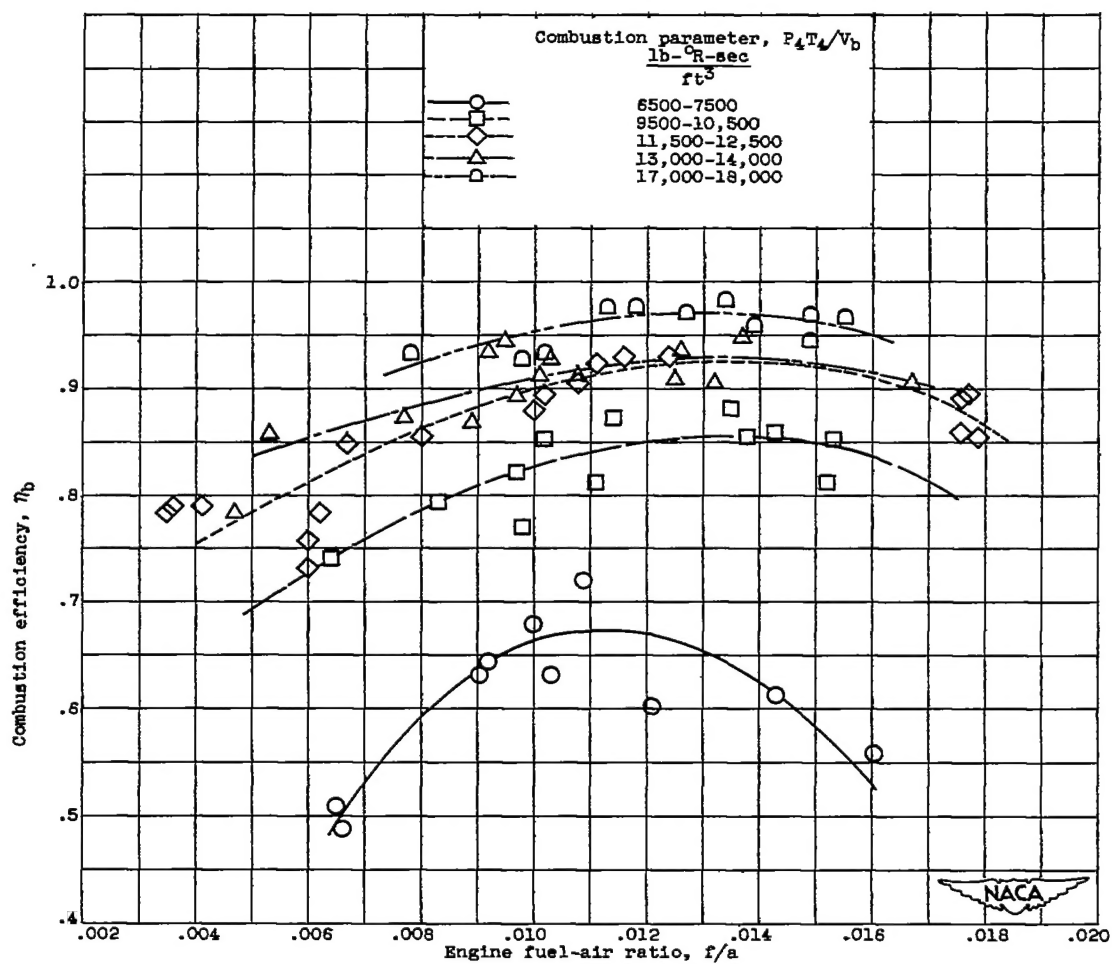


Figure 18. - Variation of combustion efficiency with fuel-air ratio for several values of combustion parameter. Compressors 1 and 2 with combustors A and B, respectively.

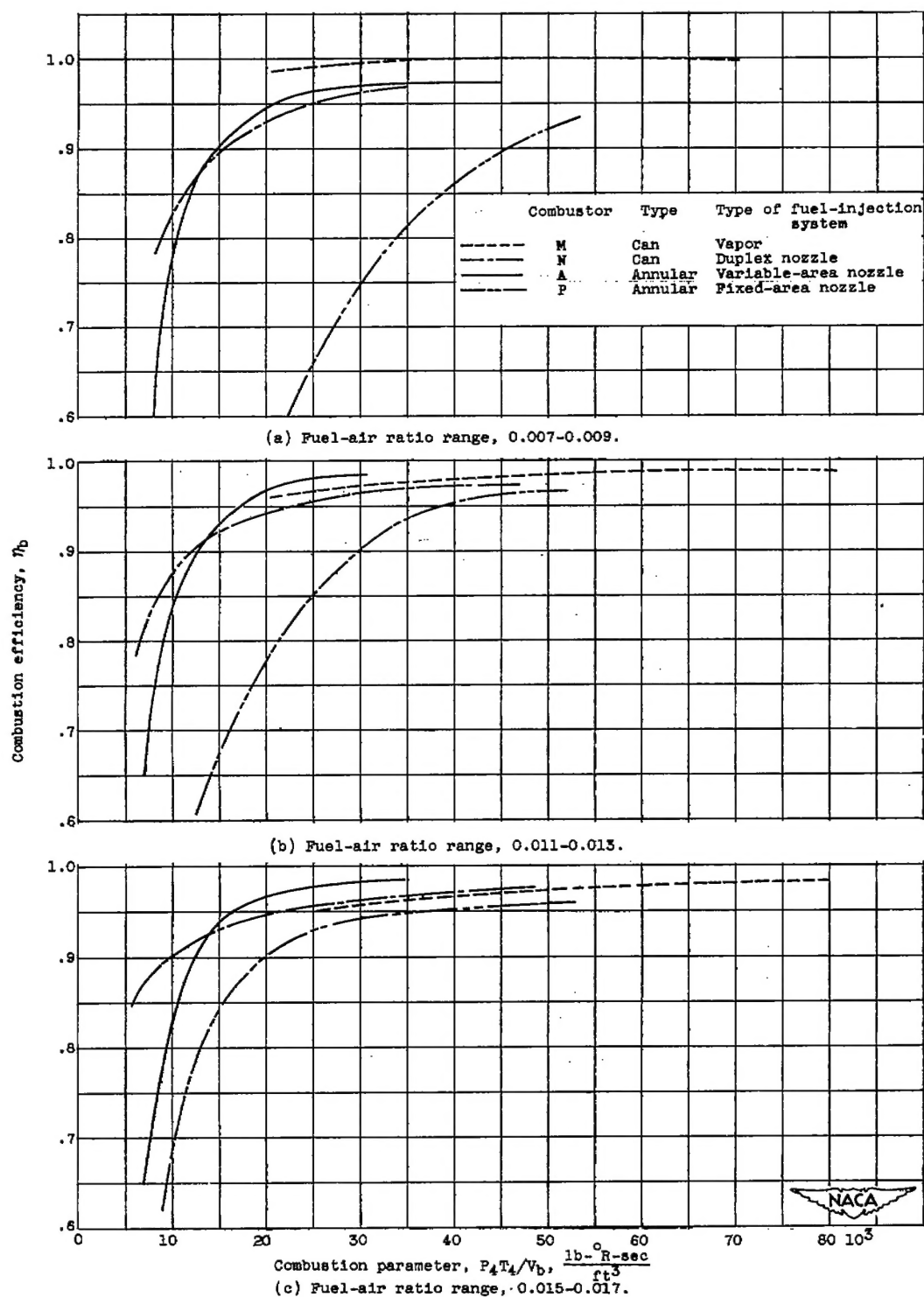


Figure 19. - Variation of combustion efficiency with combustion parameter for several unrelated combustors.

# SECURITY INFORMATION

[REDACTED]



[REDACTED]